Title

Changes in zooplankton habitat, behavior, and acoustic scattering characteristics across glider-resolved fronts in the Southern California Current System

Authors

Powell, Jesse R

Ohman, Mark D

Publication Date

2015-05-01

DOI

10.1016/j.pocean.2014.12.011

Peer reviewed

Progress in Oceanography xxx (2015) xxx–xxx

Contents lists available at ScienceDirect

Progress in Oceanography

journal homepage: www.elsevier.com/locate/pocean

Changes in zooplankton habitat, behavior, and acoustic scattering characteristics across glider-resolved fronts in the Southern California Current System

Jesse R. Powell, Mark D. Ohman *

California Current Ecosystem LTER site, Scripps Institution of Oceanography, University of California, San Diego, La Jolla, CA 92093-0218, United States

ARTICLE INFO

Article history:
Received 29 April 2014
Received in revised form 12 December 2014
Accepted 12 December 2014
Available online xxxx

ABSTRACT

We report cross-frontal changes in the characteristics of plankton proxy variables measured by autonomous *Spray* ocean gliders operating within the Southern California Current System (SCCS). A comparison of conditions across the 154 positive frontal gradients (i.e., where density of the surface layer decreased in the offshore direction) identified from six years of continuous measurements showed that waters on the denser side of the fronts typically showed higher Chl-*a* fluorescence, shallower euphotic zones, and higher acoustic backscatter than waters on the less dense side. Transitions between these regions were relatively abrupt. For positive fronts the amplitude of Diel Vertical Migration (DVM), inferred from a 3-beam 750 kHz acoustic Doppler profiler, increased offshore of fronts and covaried with optical transparency of the water column. Average interbeam variability in acoustic backscatter also changed across many positive fronts within 3 depth strata (0–150 m, 150–400 m, and 400–500 m), revealing a front-related change in the acoustic scattering characteristics of the assemblages. The extent of vertical stratification of distinct scattering assemblages was also more pronounced offshore of positive fronts. Depth-stratified zooplankton samples collected by Mocness nets corroborated the autonomous measurements, showing copepod-dominated assemblages and decreased zooplankton body sizes offshore and euphausiid-dominated assemblages with larger median body sizes inshore of major frontal features.

Introduction

Ocean fronts separate waters with different temperature, salinity and nutrient profiles. Consequently, the floral and faunal assemblages on either side of a front can diverge. Fronts, therefore, have long been thought to play an important role in spatially structuring biomass and species distributions (Lefevre, 1986; Sournia, 1994). Much of the research into the ecology of fronts, however, has focused on fronts that are either relatively persistent in time and space, such as those that occur at large-scale ocean convergences (Polovina et al., 2001), or occur predictably due to their association with continental shelf breaks (Munk et al., 2003), tides (Pingree et al., 1975), nearshore upwelling (Smith et al., 1986), or estuarine mixing (Eggleston et al., 1998). Here we assess the roles of recurrent mesoscale (O(30–300 km)) and submesoscale (O(1–10 km)) fronts in structuring marine zooplankton assemblages and habitats in deeper waters of an eastern boundary current ecosystem.

The California Current is an eastern boundary current flowing along the west coast of North America from Vancouver to Baja California (Hickey, 1979). Within the California Current System (CCS) there are three major interacting currents that transport four distinct water types. The California Current (CC) proper is an equatorward flowing surface current; the Inshore Counter Current (ICC) transports warm subtropical surface waters poleward in the nearshore region, and is strongest during the fall and winter months; and the subsurface (200–500 m), poleward California Undercurrent (CUC) transports relatively warm, high-salinity, high nutrient waters from more southern sources (Simpson, 1984; Gay and Chereskin, 2009; Todd et al., 2011). The CCS is notable for its complex and vigorous mesoscale flows, which are primarily forced by seasonal upwelling-favorable winds along the coast (Marchesiello et al., 2003). These upwelling favorable winds, and consequent Ekman transport of surface waters offshore, are also responsible for transporting subsurface cold, salty, and nutrient-rich waters into surface waters.

The CCS is therefore a patchwork of different water masses that are horizontally stirred by eddies and jets, brought in close proximity to each other, and separated by ocean fronts. This mesoscale horizontal stirring can create a mosaic of potential habitats (Martin, 2003). Within the CCS, satellite SST and ocean color imagery suggest that, over a time scale of days to weeks, phytoplankton

* Corresponding author. Tel.: +1 858 534 2754.
E-mail address: mohman@ucsd.edu (M.D. Ohman).

http://dx.doi.org/10.1016/j.pocean.2014.12.011
0079-6611/

can be considered nonconservative tracers of the flows in which they are embedded (Denman and Abbott, 1994). A dominant phytoplankton assemblage may be selected by the specific conditions in a water parcel (d'Ovidio et al., 2010). A predictable transition often occurs from waters with low surface chlorophyll (with an offshore-type assemblage) to high-surface chlorophyll (with an inshore assemblage) across the inshore edge of the low-salinity core of the California Current, approximately 100–150 km offshore (Venrick, 2009).

The zooplankton assemblages that exist in association with the varying phytoplankton assemblages might likewise differ, even though the assemblages within adjacent water parcels may be separated by a narrow front. Ship-based studies of ocean fronts in the CCS have demonstrated that zooplankton biomass and abundance can change rapidly across fronts. Mackas et al. (1991) found a 3–4-fold increase in zooplankton biomass across a cold-water filament extending offshore from Point Arena, California, with a shift from a more doliolid-dominated assemblage on the warm side of the filament to a crustacean-dominated assemblage within the filament and extending to its cold side. In the Ensenada Front within the southern CCS (SCCS), Haury et al. (1993) noted a 3-fold change in primary productivity and 3–4-fold change in zooplankton displacement volume over a distance of less than 15 km across the front. In another front in the same region (the A-Front), Ohman et al. (2012) found that abundances of calanoid copepods were elevated within the front, and detected a shift from a herbivorous, particle-grazing zooplankton assemblage on the cool side of the front to a more carnivorous-dominated assemblage on the warm side. Smith and Lane (1991) found that *Eucalanus californicus* within the Point Arena cold filament were able to maintain increased egg production without drawing down their lipid reserves, due to the increased food availability within the filament. In the A-Front study, Ohman et al. (2012) also noted an increased abundance of copepod nauplii within the front, suggesting that secondary production was elevated there. Balancing this potential for increased secondary production is the potential for increased predation risk. Fronts have long been known to attract mobile zooplanktivores, including fish (Humston et al., 2000), seabirds (Ainley et al., 2009), baleen whales (Munger et al., 2009), and turtles (Polovina et al., 2004). Increased abundances of carnivorous zooplankton such as narcomedusae can also occur at fronts (McClatchie et al., 2012).

Zooplankton within the SCCS show some general cross-shore trends in zooplankton biomass. Ohman and Wilkinson (1989) found that the ash-free dry mass of zooplankton decreased offshore along cross-shore transects within the CalCOFI survey region. Other studies have found a long-term local maximum in zooplankton displacement volume located approximately 100 km offshore, which is maintained either by advection of zooplankton-enriched waters from the north (Chelton et al., 1982), or possibly by increased secondary production fostered by wind-stress curl driven upwelling offshore (Chelton, 1982; Rykaczewski and Checkley, 2008). Johnston and Rudnick (2014) demonstrate topographically-related increased mixing at the western boundary of the Southern California Bight, which potentially could be related to increased nutrient fluxes and food web responses in the region. Offshore of the local maxima, however, average zooplankton displacement volumes decreases monotonically (Chelton, 1982; Ohman and Wilkinson, 1989). In addition to the noted biomass trends, size compositions of zooplankton assemblages also change when moving offshore, with an increasing fraction of biomass coming from smaller-bodied zooplankters (Rykaczewski and Checkley, 2008).

Our understanding of the ecological changes occurring across ocean fronts comes mostly from limited duration ship-based studies of individual fronts. To quantify the ecological changes observed across fronts within a region, it is necessary to sample a representative distribution of such features through extended studies encompassing a variety of frontal conditions over a multi-year period. The advent of autonomous ocean gliders has opened new opportunities for continuous *in situ* measurements across (sub)mesoscale features in the California Current System (Davis et al., 2008; Ohman et al., 2013). Within the SCCS, *Spray* ocean gliders revealed that horizontal gradients in physical properties (e.g., temperature, salinity, and density) co-varied with horizontal gradients in Chl-*a* fluorescence and acoustic backscatter measured at 750 kHz (Powell and Ohman, 2015). Frontal regions were more likely to be zones of elevated acoustic backscatter compared to non-frontal regions, suggesting that fronts act as zooplankton accumulation zones. In the biotic and hydrographic gradient regions, Powell and Ohman (2015) estimated that large mobile planktivorous predators were up to three-times more likely to encounter favorable foraging conditions by traveling up local density gradients rather than down those gradients.

In the present analysis, we analyze differences that occur on either side of frontal regions in the SCCS. These differences include cross-frontal changes in concentrations and the vertical distribution of phytoplankton Chl-*a*, and in acoustic characteristics, body size, taxonomic composition, and Diel Vertical Migration behavior of zooplankton assemblages. We address three questions related to glider-detected fronts in the SCCS: (1) Do the depth of the chlorophyll maximum and the depth of the euphotic zone change across fronts? (2) Does the amplitude of Diel Vertical Migration behavior change at frontal boundaries? (3) Does the size structure of zooplankton and micronekton assemblages changes across frontal transitions?

Material and methods

Study area and duration

Spray ocean gliders were deployed nearly continuously along lines 80 and 90 of the California Current Ecosystem Long-Term Ecological Research (CCE-LTER) and CalCOFI sampling area (Fig. 1) between October 2006 and July 2011. The gliders traveled autonomously along the two lines from about 20 km offshore of the coast to a maximum 370 km (line 80) and 585 km (line 90)

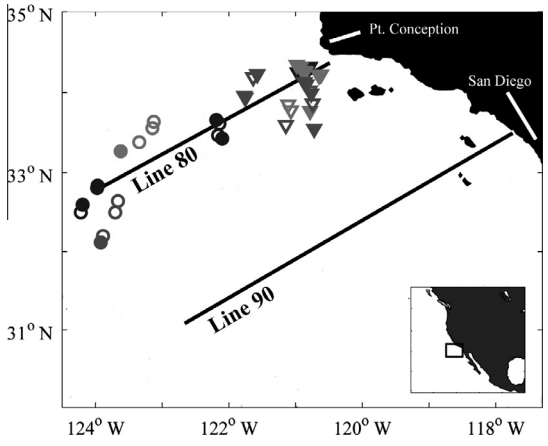

Fig. 1. CCE-LTER *Spray* glider transect lines 80 and 90, off the Southern California coast. Inset shows location off North America. Symbols depict location of Mocness tows conducted during three cruises: P0605 (black), P0704 (light gray), and P0810 (dark gray). Circles and triangles indicate tows occurring offshore and inshore, respectively, of a contemporaneous major frontal feature along line 80. Open (solid) symbols indicate daytime (nighttime) tows.

Please cite this article in press as: Powell, J.R., Ohman, M.D. Changes in zooplankton habitat, behavior, and acoustic scattering characteristics across glider-resolved fronts in the Southern California Current System. Prog. Oceanogr. (2015), http://dx.doi.org/10.1016/j.pocean.2014.12.011

offshore. A total of 124 transects was completed during the study period comprising 22,942 vertical profiles. Measurements are ongoing.

Spray glider and instrument payload

In this study, autonomous underwater *Spray* gliders (Sherman et al., 2001) were equipped with a pumped Seabird 41CP Conductivity–Temperature–Depth (CTD) sensor, SonTek 750-kHz 3-beam Acoustic Doppler Profiler (ADP), and a mini-Seapoint chlorophyll *a* fluorometer (mini-SCF). A biocide inhibited biofouling when the pump was not operating. Sensors were powered and data recorded only during ascent, apart from one ADP beam that was used as a bottom altimeter on descent. Profiles were regularly completed to a depth of 500 m approximately every 3 h for 3 months, with average inter-profile spacing of 3 km. The gliders typically traveled 25 km a day over ground, though this distance is influenced by prevailing currents.

Fluorometers were calibrated before and after each glider deployment using pure chlorophyll *a* (Sigma Life Sciences) dissolved in 90% acetone as described in Powell and Ohman (2015). We report in vivo fluorescence in standardized Chl-*a* fluorescence units (SFU), where one SFU is defined as the measured fluorescence signal (in volts) of a solution of 10 μg L^{-1} of Chl-*a* at a fixed path length (c.f., Powell and Ohman, 2015). For the fluorometers used in this study, one SFU corresponds very approximately to 2 μg Chl-*a* L^{-1}.

Each of the three acoustic beams from the SonTek ADP has a slant angle of 25° from downward upon glider ascent, and has a 3 dB beam width of 2° that samples an equivalent volume. For each profile, current velocity and acoustic backscatter (ABS) are recorded upon ascent in five 4-m vertical range bins, hence vertical resolution of the completed profile is 4 m. During each 4 m of ascent, the ADP fires one 16-ping ensemble at a ping rate of 10 Hz and records the acoustic backscatter. Acoustic backscatter is recorded as acoustic counts, which is the digitized output from a log-linear amplifier. The data from the individual pings within an ensemble are averaged to yield a single datum per beam per bin. Data from different SonTek ADPs, as well as from the same ADP used in multiple deployments, were intercomparable. Each ADP was calibrated before and after each glider mission using a standard tungsten-carbide target suspended in a test pool (see Appendix for details). The calibrations revealed an average difference in ABS recorded by an individual ADP across multiple deployments of 2.5 dB, and an average difference between different ADP instruments of 3 dB. Our horizontal gradient calculations are insensitive to such differences in instrument sensitivity.

For this study, we report acoustic results as relative Mean Volume Backscatter (MVBS) since we could not absolutely determine the source level and receiver sensitivity of each ADP, but only relative to each other. ABS counts were converted into volume backscatter, S_v, using the sonar equation $S_v = RL - SL + 2TL - 10\,\mathrm{Log}_{10}V$, where Receiver Level (RL) is the recorded ABS in dB, Source Level (SL) in decibels is set to 170 dB, Transmission Loss (TL) is equivalent to $20\,\mathrm{Log}_{10}R + \alpha R$, where R is the range in meters to the midpoint of the bin and α is the sound attenuation coefficient (dB m^{-1}), and V is the volume in cubic meters. The TL term above is indicated in the literature as the appropriate formulation for point scattering, rather than volume scattering (Medwin and Clay, 1998). However, a dataset-wide comparison of average deep backscatter (below 200 m) from the different range cells indicated that $20\,\mathrm{Log}_{10}R + \alpha R$ better corrected for spherical spreading than the conventionally recommended formulation for volume backscatter of $10\,\mathrm{Log}_{10}R + \alpha R$. Hence, we applied the $20\,\mathrm{Log}_{10}R + \alpha R$ relation. Volume backscatter data are then averaged to yield Mean Volume Backscatter (MVBS). ABS recorded by the SonTek ADP is proportional to the log of net-collected zooplankton biomass in the vicinity of the ADP (Powell and Ohman, 2012).

Although backscatter intensity from different acoustic Doppler current profilers has been used to estimate zooplankton biomass in seafloor-mounted (Flagg and Smith, 1989), vessel-mounted (e.g., Ashjian et al., 2002), and CTD-rosette profiling (Postel et al., 2007) configurations, the glider-mounted configuration that we adopt here has a number of advantages, The glider itself profiles to 500 m depth, so it is possible to record acoustic backscatter in mesopelagic depths using higher frequency transducers (750 kHz here) for which absorption would normally limit acoustic range to a few tens of meters or less. The acoustic returns are also independent of surface-associated motions typical of ship deployments. Furthermore, sampling can be directed remotely to target regions or features of interest.

Glider data processing

Data from each glider deployment were quality controlled by processing scripts or visual inspection. Data that exceeded reasonable boundaries for temperature, salinity, fluorescence, and backscatter were excluded from analysis. For example, the inlet tube for the CTD and fluorometer were, on rare occasions, temporarily blocked and salinity dropped close to zero. These data were flagged and the analyst would then confirm where the bad data began and ended. Only data from complete transects, where the glider completed 90% or more of its intended trackline, were included in the analysis. Variables included in this study include temperature, salinity, potential density, Chl-*a* fluorescence (as SFU), and acoustic backscatter (MVBS) measured within each of the three acoustic beams. For each profile within a given transect, data were vertically averaged into 5-m depth bins.

Front definition and canonical front construction

Diel periodicity in biological measurements (Cullen and Lewis, 1995; Ohman et al., 1998; Pearcy et al., 1977) makes it difficult to directly compare horizontal changes in successive glider dives. Hence, both physical and biological gradient data were calculated using an averaging approach: gradients are defined as the difference between averages of properties within the surface layer (0–50 m) from the 24 h periods before and after the glider reached a location. By definition here, a gradient is the inshore average minus the offshore average.

The locations of fronts (i.e., high horizontal density gradient zones) within any particular transect were identified objectively by an algorithm (details in Powell and Ohman, 2015). Potential fronts were defined at dives with horizontal density gradient values greater than the 95th percentile of all the gradient values for the given line (line 80: 0.0110 kg m^{-3} km^{-1} or line 90: 0.0079 kg m^{-3} km^{-1})) within the dataset, or less than the 5th percentile of all gradient values (line 80: −0.0037 kg m^{-3} km^{-1} or line 90: −0.0055 kg m^{-3} km^{-1}) for the given line within the dataset. Gradients above the 95th percentile are termed "positive" density fronts and those below the 5th percentile "negative" density fronts. If more than one contiguous dive was flagged as a potential front, the dive with the maximum (minimum) gradient value within the contiguous run of dives was denoted as a positive (negative) density front. Positive density fronts are those where near-surface density is higher on the inshore side of the front. To further analyze the average changes seen across fronts, we constructed typical, or "canonical", front sections by first aligning all glider sections containing individual positive fronts relative to the front location ($x = 0$). Our analysis of canonical fronts presents results from positive fronts because they were consistently of greater magnitude than negative fronts on both lines 80 and 90 (Powell

Please cite this article in press as: Powell, J.R., Ohman, M.D. Changes in zooplankton habitat, behavior, and acoustic scattering characteristics across glider-resolved fronts in the Southern California Current System. Prog. Oceanogr. (2015), http://dx.doi.org/10.1016/j.pocean.2014.12.011

and Ohman, 2015). All data located inshore and offshore of those frontal locations were binned by their horizontal distance from the front in 5-km increments. Vertical binning within these canonical front sections remained at 5 m. The mean value of hydrographic data within each bin was then computed to produce canonical sections of the hydrographic variables. Canonical sections of biotic variables (MVBS and SFU) were similarly derived except that MVBS and SFU data from each individual transect were first standardized to a 0–1 scale to create standardized indices of Acoustic Intensity (AI) and Fluorescent Intensity (FI), respectively. The scaled MVBS was equal to MVBS divided by the 95th percentile of MVBS values for that section, and scaled SFU was equal to SFU divided by the 98th percentile of SFU values for that section. MVBS and SFU data values above the 95th and 98th percentile, respectively, were set to 1 in the scaled variables. The reader should be aware, however, that AI cannot be interpreted on a strictly linear scale since it is calculated via the division of logarithmic units.

Interbeam differencing and smoothing algorithms

The *Spray* ADP has three acoustic beams. In addition to the mean MVBS data from all three beams, which we used as a proxy for zooplankton biomass, we also analyzed interbeam differences in MVBS in order to characterize the scattering characteristics of the assemblage. Thus, starting with unbinned volume backscatter (S_v) data, the maximum interbeam difference in volume backscatter (maxDSV) is defined as the maximum difference in recorded S_v between any two of the beams within the ADP's third range cell (16–20 m). Identical volumes of water but different patches were sampled by each of the three beams. The maxDSV for each profile was then binned into 5-m vertical bins and averaged. A smoothed and binned maxDSV section was generated for each glider transect by filtering the original maxDSV section data using a two-pass Gaussian filter weighted by 2 standard deviations. We used a kernel with a window size of five rows (i.e., five vertically contiguous depth bins) by N columns, where N equals the number of dives occurring within a 24 h window centered on the dive of interest.

While our horizontal gradient calculations are not affected by differences in instrument sensitivity (e.g., a 0.5 dB km^{-1} change across a front will likely be the same whether an ADP reports a −70 dB maximum or another reports a −72 dB maximum), our calculations of interbeam maxDSV would be affected by small variations between acoustic beams. Hence, prior to the calculation of maxDSV and MVBS, the raw ADP data from each individual transect were adjusted so that the mean response of each beam was similar. For each profile within a transect, beam-specific means of Acoustic Backscatter (ABS) measured within all depth bins in the profile were determined. The average of the three means set as the ideal response of the instrument. A transect-specific correction factor for each beam was calculated as the difference between the ideal response and the individual beam's mean response, then data from each beam were adjusted by its beam-specific correction factor. Across all data, the mean difference between beams within a transect before and after adjustment was 0.075 dB and <0.001 dB, respectively, and the standard deviation of the difference between beams within a transect before and after adjustment was 0.794 dB and <0.001 dB, respectively.

Mocness sample processing and ZooScan analysis

To compare cross-frontal acoustic changes with physical net samples, we sampled zooplankton in the same regions, but not at the same time, as the glider data. Zooplankton were collected in vertically stratified net samples with Mocness (Wiebe et al., 1985) tows (1 m^2 mouth opening, 202-μm mesh) conducted during the P0605, P0704, and P0810 process cruises of the CCE-LTER program (http://cce.lternet.edu/data/cruises/). For each cruise, Mocness tows were categorized by their location with respect to the major frontal features occurring along line 80, as identified either by *Spray* glider (P0704 and P0810) or by ship-based Moving Vessel Profiler (P0605, cf. Ohman et al., 2012). Tows were categorized as either inshore or offshore of a front (Fig. 1). However, glider and Mocness sampling did not occur concurrently in precisely the same location, so the two could not be directly compared.

For each Mocness tow, nine nets sampled zooplankton in 50-m vertical strata from 450 m to the surface. All plankton samples were preserved in 1.8% formaldehyde buffered with sodium tetraborate. Samples were then analyzed ashore using ZooScan (Gorsky et al., 2010). Prior to digital imaging with the scanner, a sample was first passed sequentially through 1000-μm and 202-μm mesh filters. The zooplankton retained on each filter were then resuspended in a measured volume of filtered seawater, and aliquots were removed from each of these size-fractionated samples for ZooScan imaging. On average 1500–2000 animals from the 202-μm size fraction and 400–700 animals from 1000-μm size fraction were imaged per scan. Initially, two scans of each size fraction were performed. However, because large-bodied zooplankters were thought to be underrepresented, a secondary set of scans using a 5000-μm mesh-filtered fraction was subsequently performed. All animals retained on the 5000-μm mesh were imaged to ensure that the large, rare zooplankters were represented in the data. To avoid double counting the larger zooplankters that might have been imaged in the original set of scans, a sample-specific zooplankter size threshold was identified for each net sample using the zooplankters' Equivalent Circular Diameter (ECD) as measured by the ZooProcess software. The size threshold was defined as the ECD value for a given net sample where the numerical abundance of zooplankters measured in the original scans dipped below the numerical abundance of zooplankters measured in the secondary scans. All data from zooplankters above this size limit present in the original scans were discarded, and the remaining data from the original and secondary scans were merged.

Each individual zooplankter was measured (ECD, area, feret length) by ImageJ routines in the ZooProcess software (Gorsky et al., 2010). The images containing individual zooplankters were then categorized into one of 20 zooplankton taxonomic categories using the Random Forest algorithm. All machine-classified images were checked manually and the classifications corrected as necessary. For presentation, the categories in this study have been aggregated into five super-categories: calanoid copepods excluding eucalanids, euphausiids, chaetognaths, eucalanid copepods (which were an optically distinctive group), and all other taxa combined. Two feature measurements, the feret diameter and the summed pixel area (or "area excluded", excluding interior voids), were used to calculate the carbon biomass of each imaged zooplankter using taxon-specific relationships from previous work in this region (extended from Lavaniegos and Ohman, 2007). The C biomass concentrations and the abundances for each of the different taxonomic categories were calculated using sample-specific metadata including sampling depth, volume filtered by the net, and fractions of samples scanned.

Estimating depth of Chl-a max and the euphotic zone

The depth of the Chl-*a* fluorescence maximum along the length of a given transect was estimated using nighttime glider profiles. Daytime profiles were not used for this purpose due to daytime non-photochemical quenching of fluorescence near the sea surface. The daytime depths of the Chl-*a* fluorescence maximum were estimated by fitting a cubic spline to the flanking nighttime data.

Euphotic zone depths were estimated from the depth at which the interpolated light level was 1% of the surface light level. The

Please cite this article in press as: Powell, J.R., Ohman, M.D. Changes in zooplankton habitat, behavior, and acoustic scattering characteristics across glider-resolved fronts in the Southern California Current System. Prog. Oceanogr. (2015), http://dx.doi.org/10.1016/j.pocean.2014.12.011

relative percent light level at the bottom of each depth bin was determined iteratively, where light level, I_{k+1}, at bin $k+1$ was calculated as:

$$I_{k+1} = I_k \times e^{-KZ_w} \quad (1)$$

where I_k is the light level at the bottom of the depth bin immediately above bin $k+1$, Z_w is the thickness of the depth bin (5 m), K is the diffuse attenuation coefficient for type I oceanic waters (Morel, 1988), defined as $K = 0.121 \times C^{0.428}$, and C is the mean chlorophyll concentration (mg m^{-3}) of the bin $k+1$ and is estimated as $C = \text{SFU} * 2$.

DVM calculations

For each glider dive, the depth of the layer of maximum acoustic backscatter was estimated by calculating the median depth of bins containing MVBS values above the 85th percentile for that dive. The amplitude of Diel Vertical Migration (DVM) for a given dive was then calculated by subtracting the median daytime scattering layer depth from the median nighttime scattering layer depth within a window that included all dives plus or minus 12 h from the given dive. The horizontal gradient in DVM amplitude at a given dive location was defined as the mean DVM amplitude occurring in a 24-h window inshore of the dive minus the mean DVM amplitude in a 24-h window offshore of the dive.

Results

Zooplankton habitat changes across fronts

A total of 154 positive fronts (i.e., inshore surface layer density > offshore surface layer density) was identified by the criterion of the upper 95th percentile of density gradients and 164 negative density fronts (offshore density > inshore density) were identified in the lower 5th percentile of density gradients. However, the positive density gradients were consistently much stronger than the negative density gradients ($p < 0.00001$ Line 80, $p < 0.01$ Line 90, Mann–Whitney U) and are therefore the primary focus of our analysis.

When transiting any particular positive front along both glider lines 80 and 90, surface waters (0–50 m) were consistently colder and saltier inshore of fronts compared with offshore (Fig. 2), though the particular hydrographic conditions of fronts and their flanking regions varied on a case by case basis. When all fronts are averaged together to create a canonical front, the density and salinity structures in regions flanking a front were markedly different in the upper 100 m (Fig. 3), with abrupt transition regions. The salinity was substantially lower offshore of the canonical front, especially in the case of line 80.

The cross-frontal changes observed in the acoustic backscatter (MVBS) and Chl-*a* fluorescence transect data (Fig. 4) were more variable than those for density or salinity. In some cases, MVBS or fluorescence increased offshore of positive fronts. However, averaged across all transects, MVBS and fluorescence values were lower offshore, as can be seen in the reconstructed canonical fronts (Fig. 5). Inshore of these fronts, MVBS was not only greater overall, but the mean vertical gradient in MVBS from the surface to 100 m was increased due to greater near surface values. There were also cross-frontal changes in both mean Chl-*a* fluorescence, and in the vertical distributions of Chl-*a* fluorescence. Offshore regions for both lines 80 and 90 exhibited a deeper subsurface maximum in Chl-*a*, whereas inshore the Chl-*a* fluorescence maximum was found closer to the surface.

Chl-a fluorescence maximum and the euphotic zone depth

As expected, the depth of the Chl-*a* fluorescence maximum generally increased with distance offshore, although in many cases the depth of Chl-*a* maximum increased and decreased multiple times along a given transect in conjunction with horizontal density gradients (e.g., Fig. 6), reflecting mesoscale and sub-mesoscale features. The median change in depth of the Chl-*a* maximum was greater when moving offshore across fronts in comparison to moving offshore in non-frontal areas (line 80: $p < 0.001$; line 90: $p < 0.001$; Fig. 7a and b). The median cross-front change in depth of the Chl-*a* maximum for line 80 and line 90 was 9.2 m and 7.9 m, respectively. Conversely, the Chl-*a* max depth shoaled in the offshore direction in the case of negative fronts ($p < 0.001$ for both lines 80 and 90; Fig. 7a and b), although the magnitude of the change was less than at positive fronts (+2.8 and +5.0 m for lines 80 and 90, respectively).

The change in depth of the modeled euphotic zone (i.e., depth at which modeled light levels are 1% those of the surface) was also greater at positive fronts compared with non-frontal areas (line 80: $p < 0.001$; line 90: $p < 0.001$; Fig. 7c and d). Euphotic zone depth was shallower at negative fronts along both lines

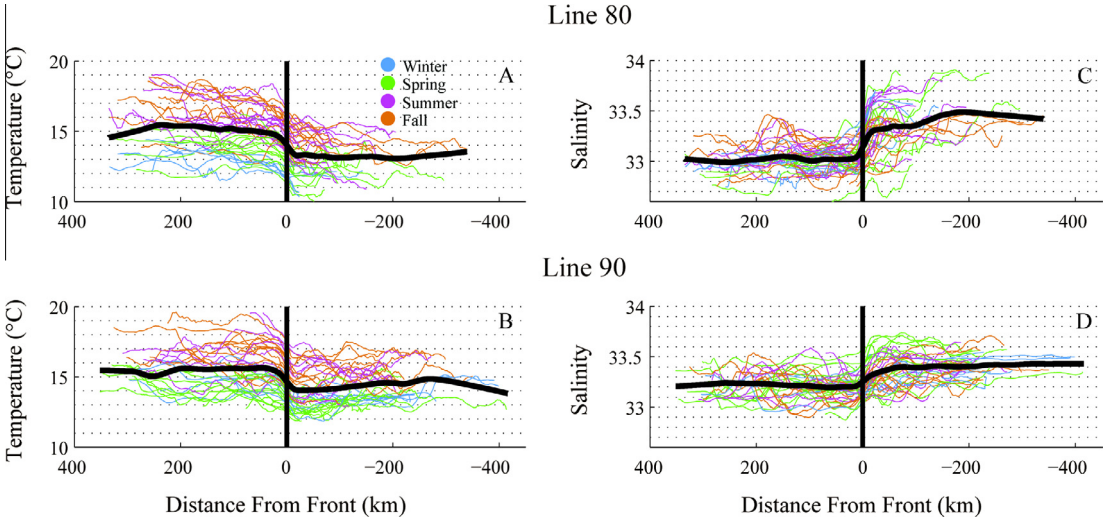

Fig. 2. Surface layer (0–50 m) (A and B) temperature and (C and D) salinity across positive fronts along (A and C) Line 80 and (B and D) Line 90. Heavy line indicates the mean. Fronts along each glider transect are aligned to 0 km. Negative distances represent distance inshore from the front, positive distances offshore from the front.

Please cite this article in press as: Powell, J.R., Ohman, M.D. Changes in zooplankton habitat, behavior, and acoustic scattering characteristics across glider-resolved fronts in the Southern California Current System. Prog. Oceanogr. (2015), http://dx.doi.org/10.1016/j.pocean.2014.12.011

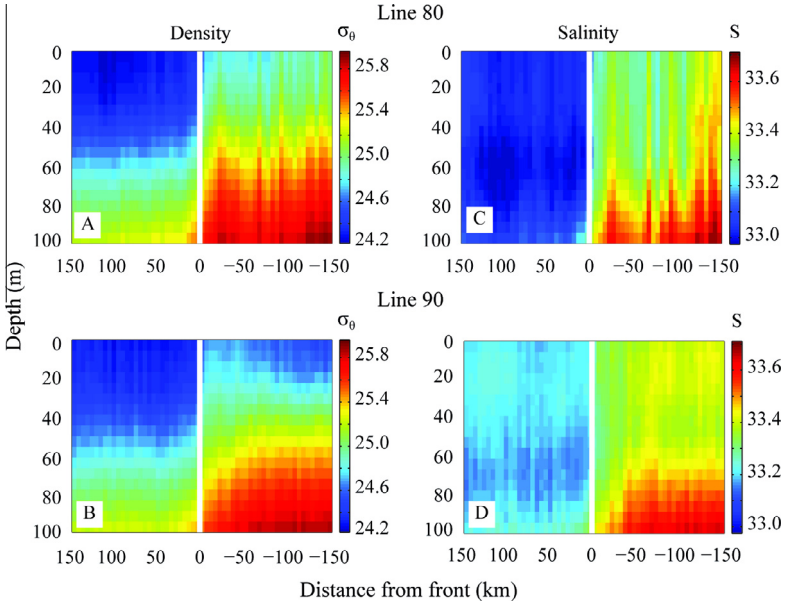

Fig. 3. (A and B) Mean density, σ_θ, and (C and D) salinity vertical structure inshore and offshore of canonical positive fronts along (A and C) Line 80 and (B and D) Line 90. Fronts along each glider transect are aligned to 0 km.

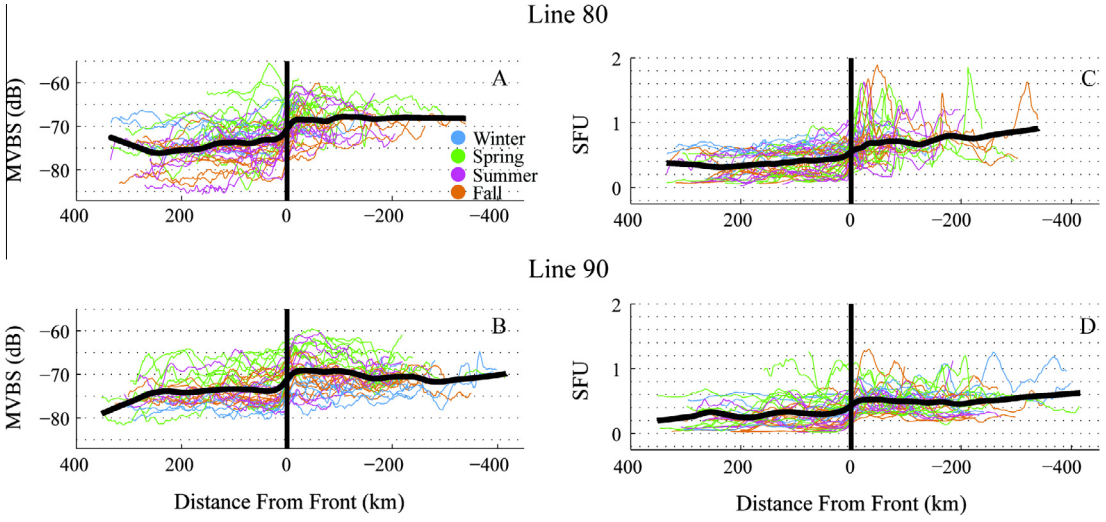

Fig. 4. Surface layer (0–50 m) (A and B) Mean Volume Backscatter (MVBS) and (C and D) Chl-*a* fluorescence across positive fronts along (A and C) Line 80 and (B and D) Line 90. Heavy line indicates the mean. Fronts along each glider transect are aligned to 0 km. Negative distances represent distance inshore from the front, positive distances offshore from the front.

($p < 0.001$; Fig. 7c and d). Euphotic zone depth was correlated with the depth of maximum Chl-*a* fluorescence ($r^2 = 0.61$; Fig. 8), suggesting that, on average, water clarity was greater offshore of fronts compared to inshore.

DVM amplitude changes across fronts

The amplitude of Diel Vertical Migration (DVM), i.e., the difference in depth between daytime and nighttime layers of maximum acoustic backscatter, was often greater offshore of fronts compared to inshore (e.g., Fig. 9). The change in DVM amplitude (Fig. 10) was greater when moving offshore across positive fronts compared to moving offshore in non-frontal areas for both line 80 ($p < 0.05$) and line 90 ($p < 0.01$). In the case of negative fronts along line 90 DVM amplitude decreased significantly ($p < 0.01$) in comparison with non-frontal areas, but not in the case of line 80 ($p > 0.05$). Again, the magnitude of changes was smaller than in the case of positive fronts. In some cases, layers of migrating animals located offshore of a front would descend 200–300 m deeper during the day compared with animals located immediately inshore of a front (cf., Fig. 9).

Across the entire dataset, DVM amplitude was non-linearly related to the modeled depth of the euphotic zone (Fig. 11). When the euphotic zone depth was shallower than 50 m, the median DVM amplitude was less than 25 m and independent of euphotic zone depth. However, when euphotic zone depths were deeper than 50 m, the median DVM increased greatly to over 200 m in some cases.

Horizontal gradients in maxDSV

Both Mean Volume Backscatter (MVBS) and beam-to-beam differences in acoustic backscatter (maxDSV; Fig. 12) are a function of the abundance and scattering characteristics of the resident faunal

Please cite this article in press as: Powell, J.R., Ohman, M.D. Changes in zooplankton habitat, behavior, and acoustic scattering characteristics across glider-resolved fronts in the Southern California Current System. Prog. Oceanogr. (2015), http://dx.doi.org/10.1016/j.pocean.2014.12.011

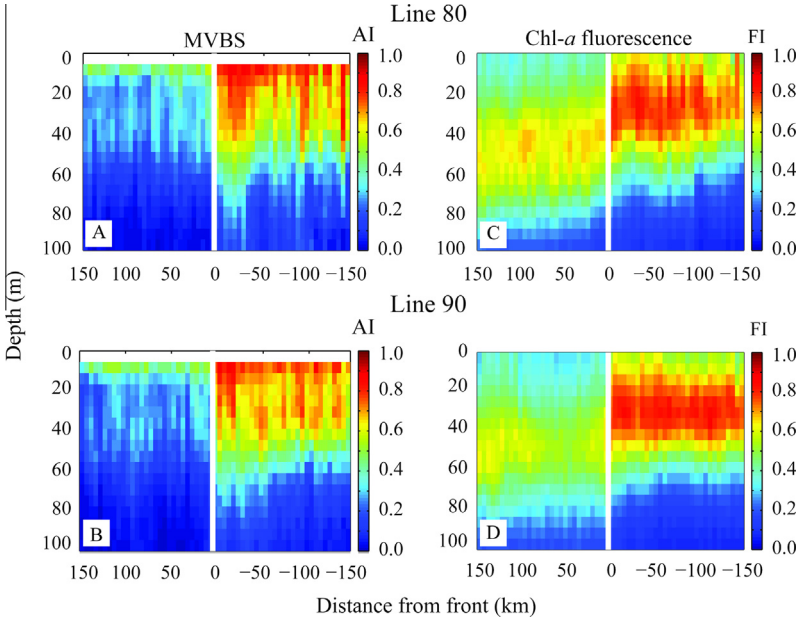

Fig. 5. (A and B) Mean Volume Backscatter (MVBS, as standardized acoustic index AI) and (C and D) Chl-*a* fluorescence (as standardized fluorescence index, FI) vertical structure inshore and offshore of canonical positive fronts for (A and C) Line 80 and (B and D) Line 90. Fronts along each glider transect are aligned to 0 km. Data are standardized to a 0–1 scale.

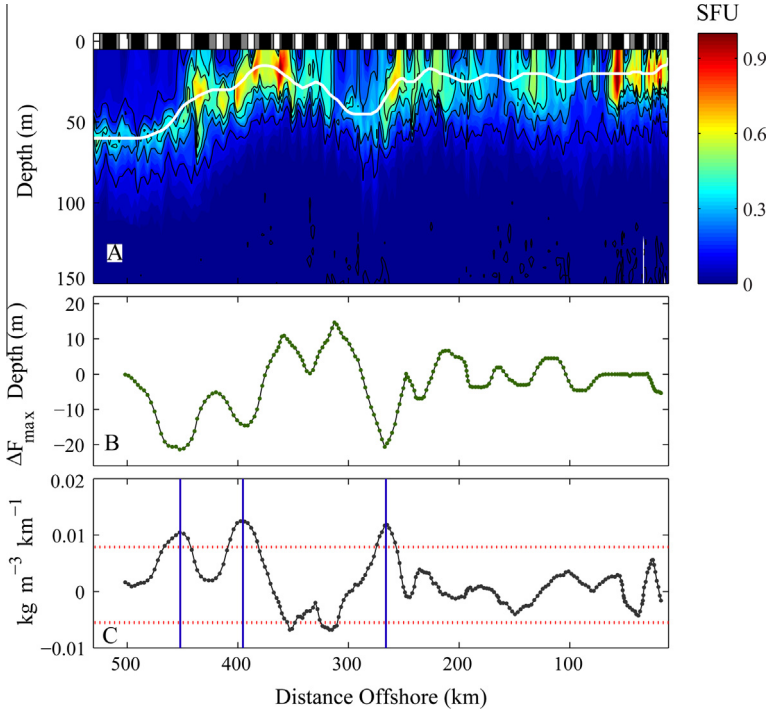

Fig. 6. Changes in the depth of Chl-*a* fluorescence maximum across ocean fronts in the Southern California Current System. (A) Vertical section of fluorescence (standardized fluorescence units, SFU) along line 90 (solid white line = depth of the Chl-*a* maximum). (B) Average change in depth of the Chl-*a* maximum, between a 24 h period inshore of given dive minus the average depth offshore of that dive. (C) Horizontal gradient in surface layer (0–50 m) density. Dotted red lines are the thresholds above or below which a front is defined. Vertical lines indicate the presence of a positive front where the average surface layer density is greater inshore than offshore. Black, gray, and white bars across top panel indicate nighttime, twilight, and daytime, respectively.

assemblage. While MVBS provides a proxy for overall biomass concentration within the specific waters ensonified by the ADP's three beams, maxDSV provides insight into how equitably the backscatter is distributed. For example, larger maxDSV values could be generated where a larger-bodied, comparatively rarer scatterer was present in only one of the beams. Thus, the size composition of the plankton field, in addition to its average biomass concentration, can influence the observed MVBS and maxDSV.

Cross-frontal changes in maxDSV were analyzed to gain insight into front-associated changes in the scattering characteristics of faunal assemblages. Fronts were sometimes associated with altered horizontal gradients in maxDSV, but only within specific

Please cite this article in press as: Powell, J.R., Ohman, M.D. Changes in zooplankton habitat, behavior, and acoustic scattering characteristics across glider-resolved fronts in the Southern California Current System. Prog. Oceanogr. (2015), http://dx.doi.org/10.1016/j.pocean.2014.12.011

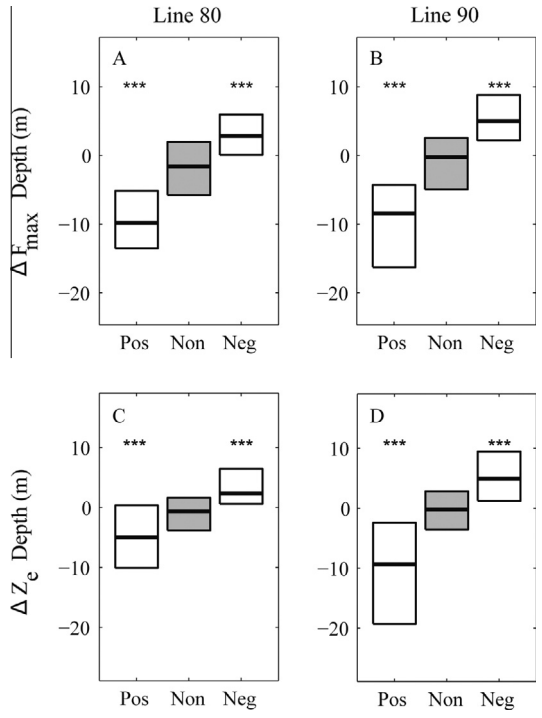

Fig. 7. Average inshore to offshore change in the depth of the (A and B) Chl-*a* fluorescence maximum and (C and D) euphotic zone across fronts compared to non-frontal regions for (A and C) line 80 and (B and D) line 90. Pos = positive density fronts, Non = non frontal regions, Neg = negative density fronts. The upper and lower boundaries of each box represent the 75th and 25th percentiles of values, respectively, and the black line the median. Asterisks indicate differences between frontal and non-frontal regions (*** = $p < 0.001$, Mann–Whitney U).

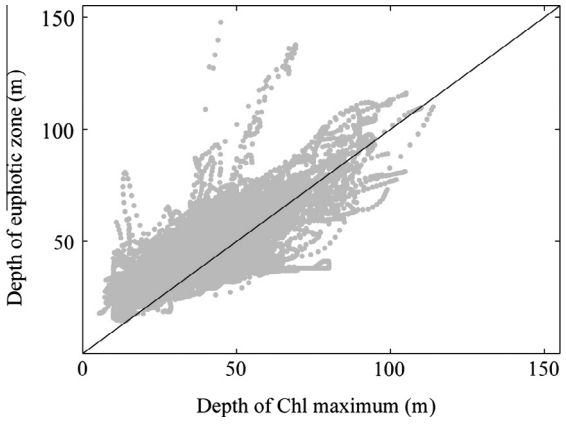

Fig. 8. Modeled depth of the euphotic zone versus the depth of the Chl-*a* maximum. Black line shows a 1:1 relationship.

depth strata (Fig. 12b). For example, along line 80, the magnitudes of horizontal gradients in maxDSV were significantly greater at fronts compared to non-frontal areas in the 400–500 m depth stratum ($p < 0.001$; Fig. 13c), indicating that maxDSV increased when moving offshore across fronts within this layer. However, no significant cross-frontal differences were observed in the 0–150 m or 150–400 m depth strata along line 80 ($p > 0.05$; Fig. 13a and b). In contrast, along line 90, the magnitudes of horizontal gradients in maxDSV were significantly greater at fronts compared to non-frontal areas in the 0–150 m and the 150–400 m depth strata ($p = 0.033$ and 0.035, respectively; Fig. 13d and e), but not within the 400–500 m stratum ($p > 0.05$; Fig. 13f). No significant changes in maxDSV were associated with negative fronts ($p > 0.05$; Fig. 13).

Glider-observed scattering characteristics (i.e., MVBS and maxDSV) also changed significantly across positive fronts within the daytime and nighttime layers of maximum acoustic backscatter. Unlike the strata mentioned above, the vertical position of these daytime and nighttime layers was not fixed, but depended on the faunal assemblages present. For both line 80 and line 90, waters inshore of positive fronts exhibited higher average MVBS and lower average maxDSV for both daytime and nighttime scattering layers (Table 1). The cross-frontal differences in both MVBS and maxDSV were more pronounced for daytime profiles than for nighttime profiles. The average cross-front changes in daytime MVBS were 6.0 and 5.8 dB for lines 80 and 90, respectively, whereas cross-front changes in nighttime MVBS were only 2.7 and 3.1 dB, respectively. All cross-front changes in MVBS were significant ($p < 0.001$). For maxDSV, the cross-front changes in daytime maxDSV were −0.24 ($p = 0.018$) and −0.33 dB ($p = 0.007$) for lines 80 and 90, respectively. In contrast, the cross-front changes in nighttime maxDSV were −0.1 dB for both lines, though only the line 90 differences were significant ($p = 0.019$).

Cross-frontal changes in water column scattering characteristics

A common feature seen in almost all transects was the occurrence of vertical layers of similar MVBS values (potentially suggesting similar biomass concentrations) but different maxDSV values (suggesting a difference in the way the biomass is distributed in the two assemblages). For example, although offshore of a front MVBS was low within both the 100–200 m and 400–500 m strata, as can be seen in Fig. 12a (light blue contours), these strata likely comprised very different scattering populations because the maxDSV values of these two layers were distinctly different (Fig. 12b).

Vertical stratification of assemblages of different scattering characteristics was somewhat more evident for waters located just offshore of fronts compared to inshore of fronts. While the MVBS of these 100–200 m and 400–500 m strata overlapped considerably, in contrast, the maxDSV values were clearly separated (Fig. 14). Offshore, the maxDSV values of the 400–500 m strata were significantly greater than those of the 100–200 m strata, for both line 80 and line 90 (Mann–Whitney U: $p < 0.001$), with a median maxDSV difference between the two strata of 1.29 dB and 1.40 dB for lines 80 and 90, respectively. Inshore, the maxDSV values of the 400–500 m strata were still significantly greater than those of the 100–200 m strata (Mann–Whitney U: $p < 0.001$), however the median maxDSV differences between the two strata were somewhat smaller than those seen offshore: 1.03 dB and 1.29 dB for lines 80 and 90, respectively.

Net samples: zooplankton assemblages and DVM

We utilized zooplankton net samples collected inshore and offshore of major frontal features to corroborate the glider-inferred cross-frontal changes in DVM behavior, and to better understand the cross-frontal changes in composition of zooplankton assemblages that might underpin the glider-observed trends in MVBS and maxDSV. Note, however, that net samples were not co-located in time and space with glider acoustic profiles.

The net samples revealed that the weighted mean depths (WMD) of zooplankton carbon biomass in daytime offshore Mocness tows were deeper than those of daytime inshore tows (Fig. 15; median WMDs = 278 m and 227 m for offshore ($N = 13$) and inshore ($N = 10$), respectively; $p < 0.001$), indicating that zooplankton were indeed migrating deeper during the day in waters offshore of major frontal features. In contrast, the nighttime WMDs did not differ significantly between inshore and offshore samples (median WMDs = 86 m and 113 m for offshore ($N = 6$) and inshore ($N = 10$), respectively; Mann–Whitney U: $p > 0.05$). Consequently,

Please cite this article in press as: Powell, J.R., Ohman, M.D. Changes in zooplankton habitat, behavior, and acoustic scattering characteristics across glider-resolved fronts in the Southern California Current System. Prog. Oceanogr. (2015), http://dx.doi.org/10.1016/j.pocean.2014.12.011

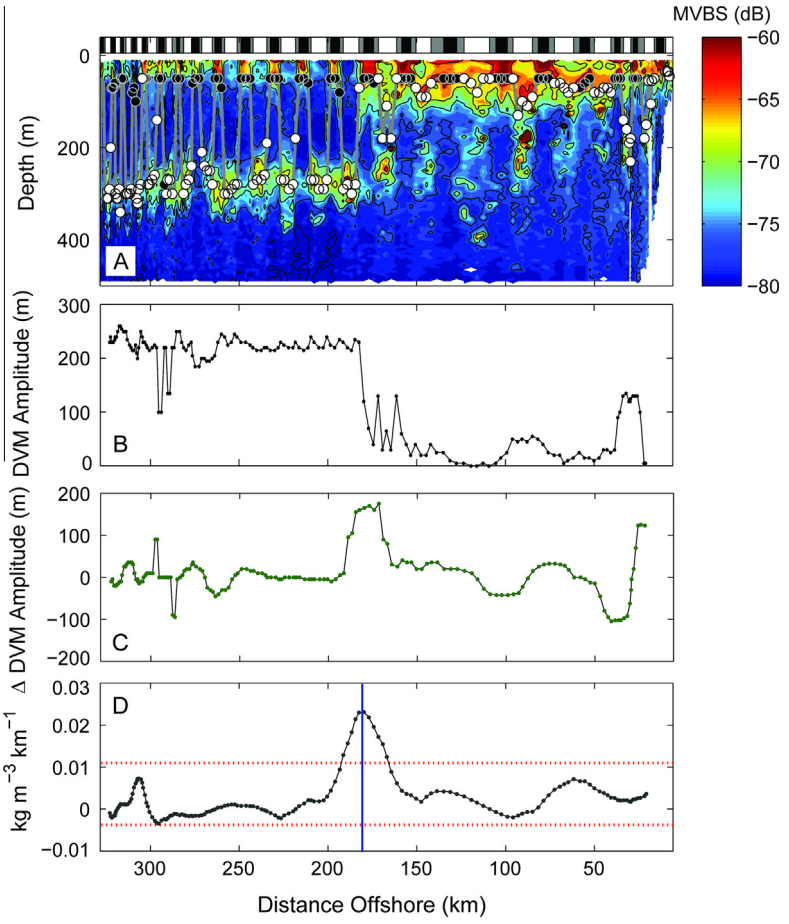

Fig. 9. Changes in Diel Vertical Migration (DVM) amplitude across ocean fronts. (A) Vertical section of Mean Volume Backscatter (MVBS) along line 80. Black (night), white (day), and gray (dawn, dusk) symbols indicate the depth the layer of maximum backscatter as the median depth of samples with MVBS values above the 85th percentile for a given dive. (B) DVM amplitude. (C) Average change in DVM amplitude between the two 24 h periods inshore and offshore of each glider dive. (D) Horizontal gradient in surface layer (0–50 m) density. Dotted red lines are the thresholds above or below which a front is defined. Vertical line indicates the presence of a positive front, where the average surface layer density is greater inshore than offshore. Black, gray, and white bars across top panel indicate nighttime, twilight, and daytime, respectively.

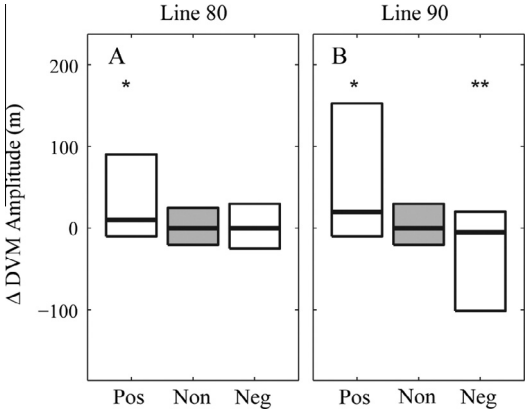

Fig. 10. Average inshore to offshore change in DVM amplitude across fronts compared to non-frontal regions for (A) line 80 and (B) line 90. Pos = positive density fronts, Non = non frontal regions, Neg = negative density fronts. Boxplots as in Fig. 7. Asterisks indicate differences between frontal and non-frontal regions (* = $p < 0.05$, ** = $p < 0.01$, Mann–Whitney U).

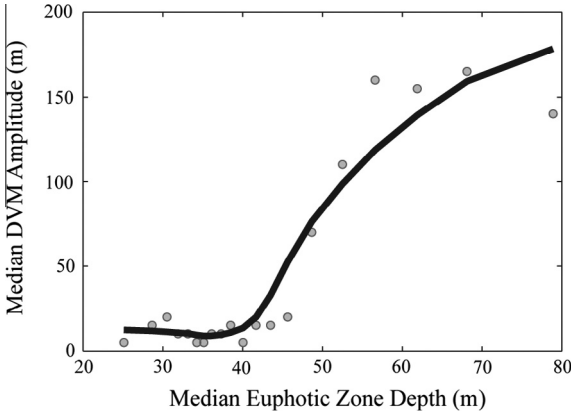

Fig. 11. Relationship between median DVM amplitude and the median depth of the euphotic zone. The modeled depth of the euphotic zone (i.e., the 1% light level) of all dives was binned into twenty 5 percentile-wide bins. Gray dots indicate the euphotic zone depth and median DVM amplitude of dives within each bin. The black line is a Lowess fit (span = 10).

the median of offshore DVM amplitudes (i.e., all possible pairwise differences between daytime and nighttime WMDs) was greater than the median of inshore DVM amplitudes (182 m versus 98 m for offshore and inshore, respectively; Mann–Whitney U: $p < 0.001$).

The taxonomic composition of zooplankton assemblages within the net samples also differed between inshore and offshore samples (Figs. 16 and 17). Our analysis focuses on data from nighttime samples because they are less susceptible to bias due to net avoidance. In nighttime zooplankton samples including all taxa

Please cite this article in press as: Powell, J.R., Ohman, M.D. Changes in zooplankton habitat, behavior, and acoustic scattering characteristics across glider-resolved fronts in the Southern California Current System. Prog. Oceanogr. (2015), http://dx.doi.org/10.1016/j.pocean.2014.12.011

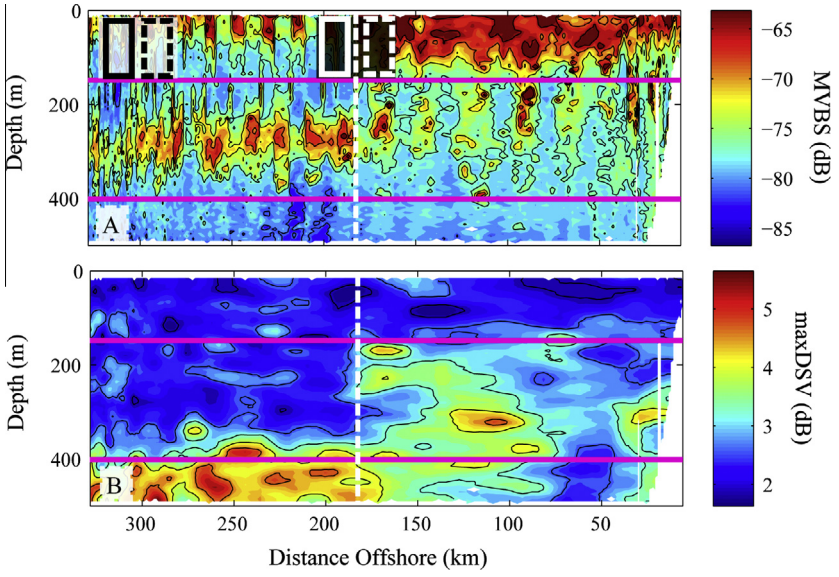

Fig. 12. Vertical sections of (A) Mean Volume Backscatter (MVBS) and (B) maximum interbeam difference in volume backscatter (maxDSV) values along a line 80 transect. The position of a front is indicated by the dotted white line. Horizontal magenta lines separate three depth strata (0–150 m, 150–400 m, and 400–500 m) that are analyzed further in Fig. 13. Boxes indicate the extent of data used to calculate average maxDSV inshore of each dive (dashed line box) and offshore (solid line box), and to compare horizontal changes in maxDSV across frontal regions (white-lined boxes) with non-frontal regions (black-lined boxes).

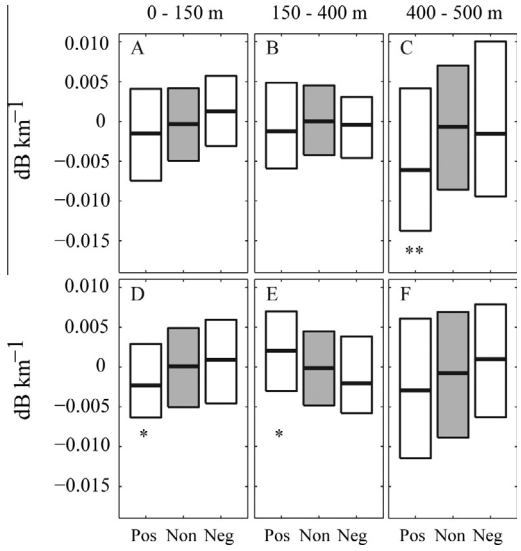

Fig. 13. Horizontal gradients in maximum interbeam difference in acoustic volume backscatter (maxDSV, dB km^{-1}) across frontal regions (open boxes) versus non-frontal regions (shaded boxes) for (A–C) line 80 and (D–F) line 90, for three depth strata (indicated above the panels). Pos = positive density fronts, Non = non frontal regions, Neg = negative density fronts. Boxplots as in Fig. 7. Asterisks indicate significant differences in the horizontal gradient at frontal regions compared to non-frontal regions (* = $p < 0.05$, ** = $p < 0.01$).

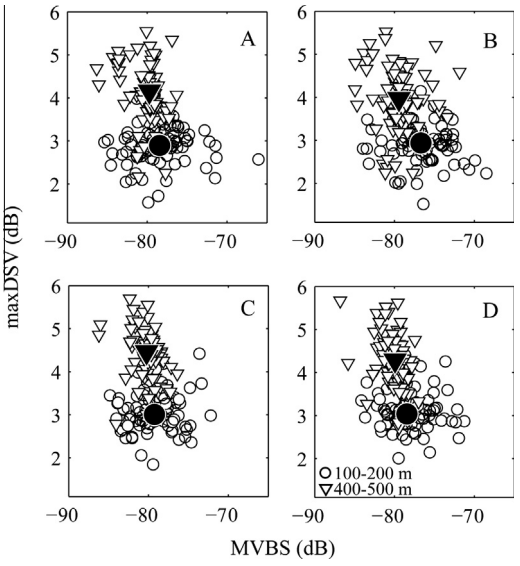

Fig. 14. Acoustic backscattering characteristics of different depth strata (A and C) offshore, and (B and D) inshore of (A and B) line 80 positive fronts ($N = 81$), and (C and D) line 90 positive fronts ($N = 73$). Open triangles (400–500 m) and circles (100–200 m) show the median MVBS and maxDSV within a specific depth stratum adjacent to a front. Filled triangles and circles show the overall median of all individual measurements from 400 to 500 m and 100 to 200 m, respectively.

Table 1
Comparison of inshore and offshore (relative to positive frontal location) scattering characteristics of daytime and nighttime layers of maximum backscatter.

	Line 80			Line 90		
	Inshore	Offshore	*p*-Value	Inshore	Offshore	*p*-Value
Daytime MVBS (dB)	−69.1	−75.1	<0.001	−71.7	−77.5	<0.001
Daytime maxDSV (dB)	2.31	2.55	0.018	2.46	2.79	0.007
Nighttime MVBS (dB)	−65.5	−68.2	<0.001	−67.4	−70.5	<0.001
Nighttime maxDSV (dB)	2.3	2.4	0.073	2.4	2.5	0.019

Please cite this article in press as: Powell, J.R., Ohman, M.D. Changes in zooplankton habitat, behavior, and acoustic scattering characteristics across glider-resolved fronts in the Southern California Current System. Prog. Oceanogr. (2015), http://dx.doi.org/10.1016/j.pocean.2014.12.011

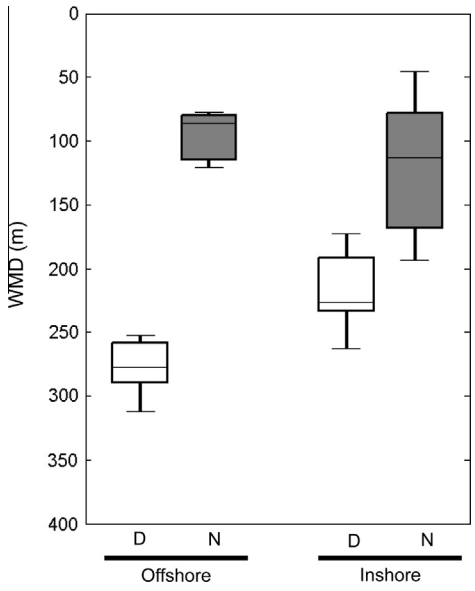

Fig. 15. Day (D, open) and Night (N, filled) weighted mean depths (WMD) of zooplankton in the offshore and inshore regions. Box plots show WMD of zooplankton collected by Mocness offshore by day ($N = 10$) and night ($N = 6$) and of zooplankton collected inshore by day ($N = 13$) and night ($N = 10$).

(Fig. 16A–F), calanoid copepods (excluding eucalanids) contributed the most biomass of any taxonomic group on a percentage basis (median 48.7% and 71.0% for inshore and offshore samples, respectively). However, we also considered only zooplankters with an ECD greater than 1.6 mm (Fig. 16G–L), which, are expected to scatter sound at 750 kHz ($\lambda = 2$ mm) more effectively than smaller-bodied zooplankters. We previously verified this expectation empirically (Powell and Ohman, 2012). Among the >1.6 mm ECD organisms calanoid copepods remained the dominant taxonomic group offshore (median = 75% of biomass), but they contributed significantly less ($p = 0.031$; Mann–Whitney U) biomass inshore (median = 21.3%) compared with the dominant inshore taxonomic group, euphausiids (median = 36.5%).

The size distribution of zooplankton found within the net samples also differed between inshore and offshore samples (Figs. 18 and 19). Inshore, zooplankters with ECDs greater than 3.8 mm contributed a greater percentage of nighttime biomass compared with offshore zooplankters (25.8% versus 5.8%, respectively), and inshore, zooplankters with ECDs greater than 8.5 mm contributed a greater percentage of nighttime biomass compared with offshore zooplankters (9.5% versus 2.7%, respectively). The percentage of biomass contributed by each size class varied substantially from sample to sample (Fig. 19). However, when all net samples were considered, the percent of nighttime biomass found inshore in the two largest size classes was significantly greater than that of

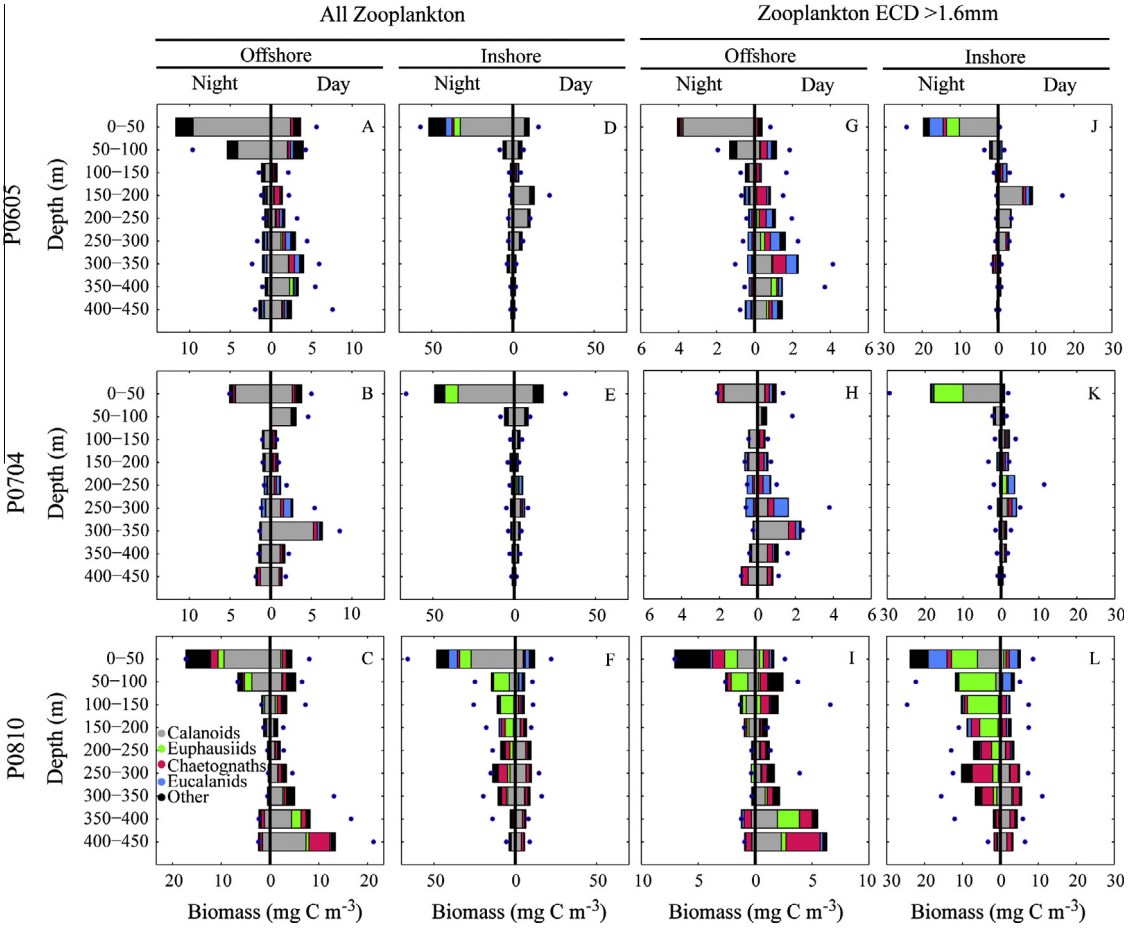

Fig. 16. Night and day vertical distributions of carbon biomass of major zooplankton taxa in the inshore and offshore regions on three cruises: P0605, P0704, P0810. The depth distributions of (A–F) all zooplankters, and (G–L) zooplankters with an ECD greater than 1.6 mm for (A–C and G–I) offshore and (D–F and J–L) inshore Mocness tows. Each bar shows the median carbon biomass concentration of all Mocness nets collected from the indicated depth stratum. Divisions within each bar indicate the mean percentage of biomass that was contributed by each major taxonomic group (calanoid copepods excluding eucalanids, euphausiids, eucalanid copepods, chaetognaths, and all others). Blue dots accompanying each bar indicate the maximum biomass value recorded at that depth. Note that horizontal scales differ.

Please cite this article in press as: Powell, J.R., Ohman, M.D. Changes in zooplankton habitat, behavior, and acoustic scattering characteristics across glider-resolved fronts in the Southern California Current System. Prog. Oceanogr. (2015), http://dx.doi.org/10.1016/j.pocean.2014.12.011

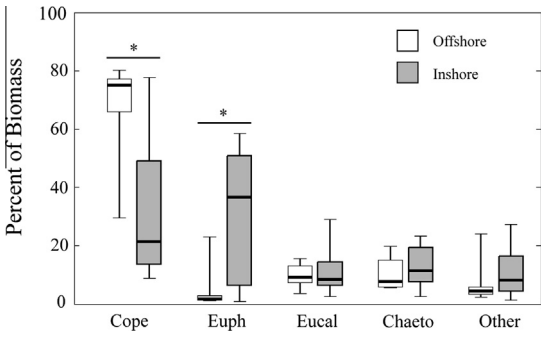

Fig. 17. Comparison of inshore and offshore carbon biomass contributions of different taxonomic groups for the three cruises combined (P0605, P0704, P0810). Boxplots shows the percent of biomass contributed to total nighttime biomass by a taxon (calanoid copepods excluding eucalanids, euphausiids, eucalanid copepods, chaetognaths, and all others) for inshore tows ($N = 10$) and offshore tows ($N = 6$). Boxplots as in Fig. 7. Asterisks indicate significant differences ($p < 0.05$; Mann–Whitney U test) between inshore and offshore percent biomass contributions for that taxonomic group.

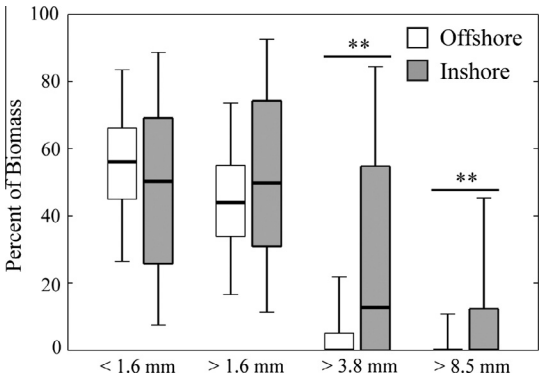

Fig. 19. Comparison of inshore (filled) and offshore (open) carbon biomass contributions of different size classes for three cruises combined (P0605, P0704, P0810). Boxplots shows the percent of biomass contributed to total nighttime biomass by a size class for inshore net samples ($N = 89$) and offshore net samples ($N = 45$). Each box spans the 25th to 75th percentile range of biomass contributions, upper and lower whiskers show the 95th and 5th percentile, and the black line within each box shows the median value. Double asterisks indicate $p < 0.001$ (Mann–Whitney U test) between inshore and offshore percent biomass contributions for that size class. Absence of asterisk indicates $p > 0.05$.

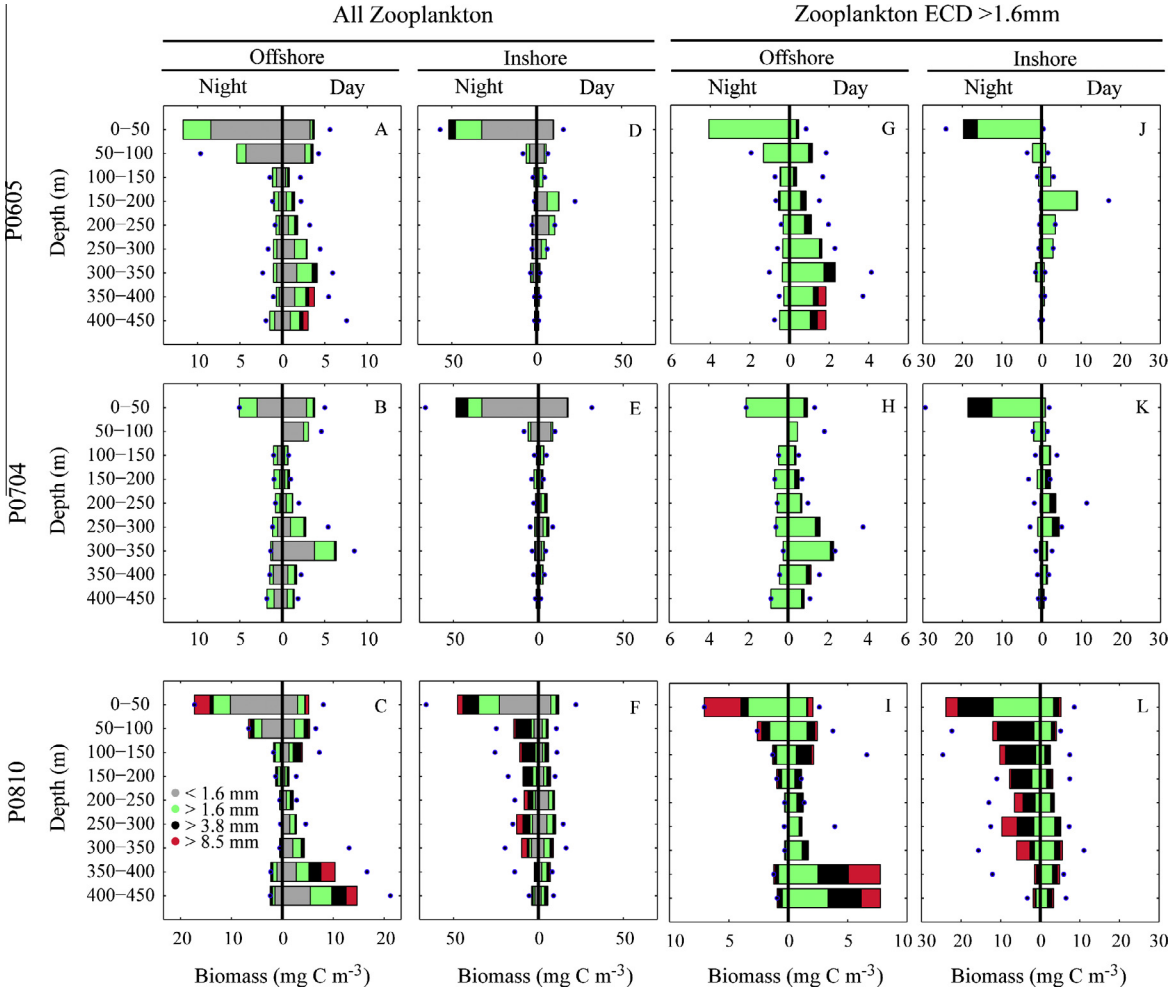

Fig. 18. Night and day vertical distributions of carbon biomass for different zooplankton size categories in the inshore and offshore regions on three cruises: P0605, P0704, P0810. The depth distributions of (A–F) all zooplankters, and (G–L) zooplankters with an ECD greater than 1.6 mm for (A–C and G–I) offshore and (D–F and J–L) inshore Mocness tows. Each bar shows the median carbon biomass concentration of all Mocness nets collected from the indicated depth stratum. Divisions within each bar indicate the mean percentage of biomass that was contributed by each size category. Blue dots accompanying each bar indicate the maximum biomass value recorded at that depth. Note that horizontal scales differ.

Please cite this article in press as: Powell, J.R., Ohman, M.D. Changes in zooplankton habitat, behavior, and acoustic scattering characteristics across glider-resolved fronts in the Southern California Current System. Prog. Oceanogr. (2015), http://dx.doi.org/10.1016/j.pocean.2014.12.011

biomass found offshore in those same size classes ($p < 0.001$ for both cases; Mann–Whitney U test).

Discussion

Our analysis of six years of autonomous glider measurements along lines 80 and 90 revealed that there were consistent ecological changes occurring across frontal boundaries in the Southern California Current System (SCCS). The depths of the Chl-*a* fluorescence maximum and the euphotic zone were deeper on the less dense side of objectively-defined fronts compared to the denser side of fronts, whether the denser waters were onshore or offshore of the frontal position. Horizontal gradients in these two properties were also steeper across fronts than in non-frontal regions. Diel Vertical Migration (DVM) amplitudes were greater on the offshore side of positive fronts compared to the inshore side, and horizontal gradients in DVM amplitudes were generally greater across fronts compared to non-frontal regions.

In concert with these changes, acoustic scattering characteristics of the faunal assemblages differed across these fronts. The inshore-to-offshore gradients in acoustic backscatter and interbeam difference in volume backscatter (maxDSV) were both enhanced across fronts compared to non-frontal areas. Net samples corroborated that inshore assemblages contained proportionately more large-bodied zooplankters than do the offshore assemblages.

Many of these observed cross-frontal ecological or habitat changes may be linked to the underlying hydrographic differences of waters found inshore and offshore of fronts. For example, the depth of subsurface chlorophyll maxima in the SCCS is primarily determined by available light and nutrient levels (Cullen and Eppley, 1981; Aksnes et al., 2007). It is likely that the deeper fluorescence maxima and deeper euphotic zones seen on the less dense side of fronts are directly related to altered nutrient concentrations and vertical distributions (Aksnes et al., 2007). By definition, the positive fronts described in this study are areas with shoaling isopycnals, and therefore are areas where nutrients are brought closer to the surface on the inshore side of fronts. The cross-frontal changes in the depth of fluorescence maxima may also be due, in part, to mechanisms such as subduction. A study of ocean mixing within the CCS using *Spray* gliders (Johnston et al., 2011), found elevated mixing rates due to internal tides and inertial waves occurring in same areas along line 80 (mostly closer to shore) and line 90 (further offshore, and centered over the Santa Rosa-Cortes Ridge, Johnston and Rudnick, 2014) where a maximum of front occurrence was reported by Powell and Ohman (2015). The increased mixing found in these locations clearly increases the potential for elevated nutrient fluxes.

It is not surprising that the stronger fronts in this region were positive fronts according to our sign convention (i.e., denser waters closer to the coast), as this is a basic constraint of geostrophy in an eastern boundary current region. Negative fronts (i.e., denser waters further from the coast) probably arise as eddies and mesoscale stirring lead to offshore transport of denser water parcels, with development of associated filaments and other frontal boundaries.

Floristically, Hayward and Venrick (1998) found that the inshore edge of the low-salinity core of the California Current often marked a sharp boundary between an offshore and inshore phytoplankton community. The offshore community is often dominated by dinoflagellates and coccolithophorids while the inshore community is dominated by diatoms (Venrick, 2002, 2009). Venrick also found that standing stocks of inshore communities were more variable than offshore communities, and that inshore community standing stocks were also more seasonal, with a springtime maximum, while the offshore standing stocks showed little seasonality. Furthermore, shoaling nitraclines, as would be found at the inshore edge of the California Current jet, have been shown to be positively correlated with increasing biomass of large (>8 μm) phytoplankton (Mullin, 1998). Our glider-based observations of vertical distributions of Chl-*a* fluorescence complement these authors' view of SCCS phytoplankton distributions.

The increased Diel Vertical Migration (DVM) amplitude that we observed offshore of fronts (in both glider acoustic data and Mocness net samples) may be associated with the cross-frontal changes in phytoplankton biomass, its vertical distribution, and associated changes in optical properties of the water column. Many studies have shown that DVM is primarily an adaptive response to predation pressure (Lampert, 1989; Ohman, 1990; De Robertis et al., 2000). Consequently, animal responses are strongly affected by ambient light levels and the associated risk of predation due to sight-hunting predators. In the present study, zooplankton prey are more likely to be vulnerable during the day to visually-hunting predators in waters offshore of fronts, where euphotic zones are deeper and waters clearer, and therefore most likely to adjust their behavior and increase daytime migrations accordingly. However, we also found that the relationship between DVM amplitude and modeled water clarity was non-linear. Glider-observed DVM amplitudes did not increase appreciably until the estimated depth of the euphotic zone surpassed 40–50 m. There may be a threshold light level for triggering increased DVM amplitudes, or factors in addition to ambient light levels may influence DVM behavior. Inspection of dissolved oxygen profiles associated with the Mocness tows showed that changes in DVM occurred at depths well above the oxygen minimum zone and appeared to be little affected by it.

One such additional factor may be that different DVM behaviors reflect the occurrence of different species across frontal boundaries. While it is not possible to identify assemblage composition by glider-observed acoustic backscatter alone, several lines of evidence support the hypothesis that the composition of the assemblage changed across these fronts. Cross-frontal changes in the maximum interbeam difference in acoustic backscatter (maxDSV) within the 400–500 m depth stratum along line 80, and the 0–150 m and 150–400 depth strata along line 90, suggest that the size composition or species composition of the assemblages may change across fronts. We also found that Mean Volume Backscatter (MVBS) decreased and maxDSV increased offshore of fronts for both the daytime and nighttime layers of maximum backscatter, again suggesting a shift in the composition of scattering assemblages. The relationship between MVBS, maxDSV, total biomass, and the size composition of the plankton field is complex. For example, one cannot assume that because maxDSV values are elevated that the size distribution of the assemblage is necessarily shifted toward larger-bodied zooplankton. However, a combined Monte Carlo simulation and inverse modeling approach using these data indicated that the size distribution of inshore assemblages is, in this case, shifted toward larger-bodied zooplankton (Powell, 2013).

Results from Mocness net tows, although sampled at different times and locations from the gliders (though within the same general region), support these interpretations. Integrated zooplankton biomass in the net samples was greater inshore than offshore, and larger-bodied zooplankters within the inshore assemblage, especially within the two largest size classes (>3.8 mm, and >8.5 mm), contributed more biomass proportionally to the total biomass compared with the offshore assemblage. Furthermore, the composition of assemblages of higher taxonomic groups shifted from a more copepod-dominated assemblage offshore to a more euphausiid-dominated assemblage inshore. Other studies within the SCCS corroborate these results, having shown a positive relationship between increased upwelling (as would be more likely

Please cite this article in press as: Powell, J.R., Ohman, M.D. Changes in zooplankton habitat, behavior, and acoustic scattering characteristics across glider-resolved fronts in the Southern California Current System. Prog. Oceanogr. (2015), http://dx.doi.org/10.1016/j.pocean.2014.12.011

to be found inshore compared with offshore) and flatter size spectra of net-collected zooplankton (Rykaczewski and Checkley, 2008).

We also found increased vertical stratification of distinct acoustic scattering layers in waters offshore of fronts compared to inshore of fronts. A notable feature in offshore waters, in particular, was the presence of a mid-depth scattering layer (often found between 250 and 350 m) with relatively high backscatter and low beam-to-beam variability located above a layer at 400–500 m with low backscatter and high beam-to-beam variability (Fig. 12). Diel backscatter patterns in this mid-depth scattering layer suggest that the layer contained mostly migratory animals, whereas the deeper layer just below appeared to be non-migratory. Comparing the scattering characteristics of the migratory layer with the non-migratory layer, it seems likely that the shallower, migratory layer is composed of more numerous, but smaller-bodied scatterers that are more evenly distributed at the fine scale. In contrast, the deeper, non-migratory layer is most likely composed of fewer, but larger scatterers which, due to their low abundance, are more variably sampled by the acoustic beams of the ADP.

Although it is possible that the deep layer of large but rare scatterers might be composed of zooplankton taxa such as pteropods, which are known to scatter sound much more efficiently than other zooplankters of equivalent biomass and dimensions (Stanton et al., 1998), the pervasiveness of the deep layer over many glider deployments implies a taxonomic group less subject to the intermittent occurrences than typify pteropods. Mesopelagic micronekton (primarily myctophids and the gonostomatids *Cyclothone* spp.) are a more likely candidate group to comprise the layer. Mesopelagic micronekton are abundant in the deep sea (Pearcy et al., 1977), and many non-migratory species remain at depths between 400 and 1000 m during the night and day in our study region (Davison, 2011). Even among some of the more abundant migratory species (e.g., *Stenobrachius leucopsarus*), a significant fraction does not participate daily in DVM (Pearcy et al., 1977). Mesopelagic fish are also likely to be strong acoustic scatterers since many species either contain swimbladders throughout their lives, or at least during their juvenile forms (Davison, 2011), so that a single animal ensonified by one of the three beams would yield a high maxDSV value. Other studies have also found that deep layers of non-migratory fish underlie daytime layers of migratory zooplankton in the Mediterranean (Andersen et al., 2004). While mesopelagic fishes may also occasionally contribute to the somewhat shallower, migratory layer seen in our acoustic records, the relatively small acoustic volume ensonified by the glider ADP, the consistency of occurrence of the mid-water layer, and the agreement of the patterns from our Mocness zooplankton analyses with acoustic backscatter results (both the present study and those in Powell and Ohman, 2012), suggest that the shallower-dwelling migrators are principally mesozooplankton scatterers.

Taken together, the cross-frontal changes in the vertical distribution of Chl-*a* fluorescence, euphotic zone depth, DVM behavior, acoustic backscattering characteristics, and the size and taxa composition of zooplankton assemblages indicate that fronts in the Southern California Current System often delineate waters with very different ecosystem characteristics beyond simple hydrographic variables. While individual ocean fronts may be ephemeral, and the biotic responses to those fronts may vary, the general picture of fronts in the SCCS that emerges from these sustained observations is one of fronts acting as ecotones, where species assemblages from the two habitats interact across an environmental gradient. Much of the existing ocean front research examines the importance of fronts with regards to specific processes such as primary productivity, advective plankton accumulation (Franks, 1992), or foraging by apex predators (Bost et al., 2009). An interesting direction for future research into ocean fronts will be to analyze how they function in a framework of landscape ecology, especially in terms of edge effects. Terrestrial ecologists have long been interested in edge effects in landscape and community ecology, and especially in their role in habitat fragmentation and conservation, and how they affect species diversity and abundance patterns. Decades of edge effect studies have begun to coalesce into a general ecological theory of edges (Ries et al., 2004). The effect of edges and boundaries in marine settings is less well understood. Unlike terrestrial ecology, where boundaries are often static at timescales relevant to the lifespan of the local species assemblages, marine boundaries are dynamic and intermittent. Nonetheless, it is clear that some species (e.g., mobile predators) have evolved strategies to seek out these structures. Are there predictable broader, perhaps community-level responses to ocean fronts as well? In this study we have shown predictable habitat changes across fronts in an eastern boundary current upwelling ecosystem. It remains to be seen to what degree such changes drive altered marine community patterns.

Acknowledgements

We thank R. Davis, D. Rudnick, R. Todd, and J. Sherman for the provision of *Spray* glider data and assistance. We also thank R. Davis, P. Franks, M. Landry, and the anonymous reviewers for comments on this manuscript. J.-B. Romagnan assisted with ZooScan analyses. Support for this work was provided by NSF via the California Current Ecosystem LTER site, and by the Gordon and Betty Moore Foundation. Glider observations were also supported by the NOAA Ocean Climate Observation Program through the Consortium on the Ocean's Role in Climate, and by the US Integrated Ocean Observation System through the Southern California Coastal Ocean Observing System (SCCOOS).

Appendix

ADP calibration protocols

The *Spray* glider Acoustic Doppler Profiler (ADP) was specially designed for the *Spray* by SonTek YSI, Inc. to measure current velocities. Since the *Spray* ADP was used here as an echosounder to map and quantify zooplankton distributions, we developed protocols to test ADP's in an instrument test pool at the Scripps Institution of Oceanography before and after each glider deployment. The purpose of these protocols is to (1) for each transducer, measure the acoustic backscatter (ABS) from a known target located in the center of the acoustic beam at a fixed distance from the ADP, (2) record the beam pattern for each transducer, and (3) to discover any potential problems with an ADP before deployment (see Fig. A1).

Calibration setup

The ADP is tested in an oval-shaped, freshwater pool whose interior dimensions are 5.5 m width, 12.5 m length and a minimum 4 m in depth. Prior to instrument calibration, the pool pumps are turned off and the pool is allowed to de-gas for at least 12 h.

At one end of the pool (e.g., approximately 3 m from the one end of the oval), the ADP is suspended from an aluminum beam 1.5 m below the surface, along the long-axis of the pool. The ADP is mounted in a bracket so that the beam being tested is aligned along the long axis of the pool, and is parallel to the water's surface.

At a distance of 5 m from the ADP transducer face, a computer-controlled X–Y stepper motor stage is mounted to a wooden bridge spanning the pool. The target sphere (a 1 cm tungsten-carbide ball)

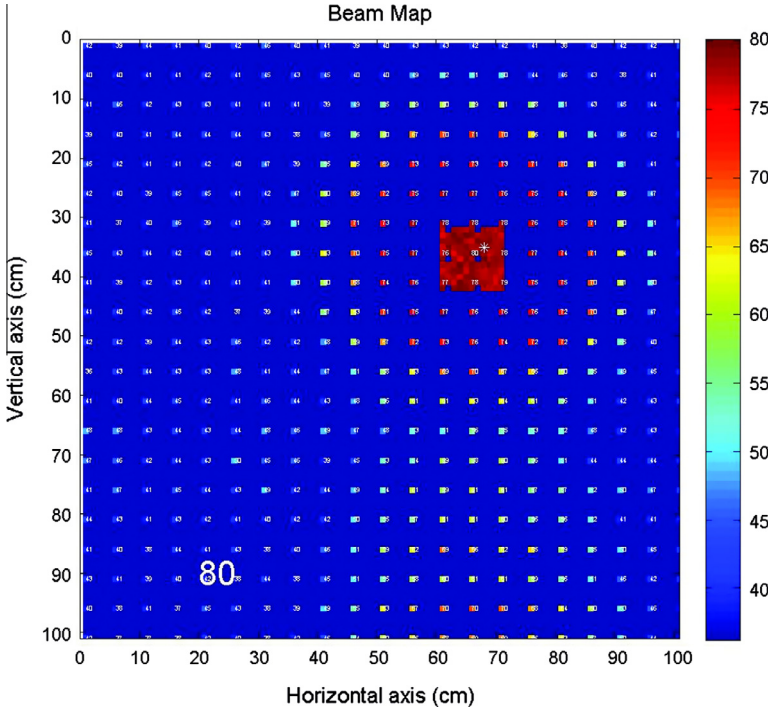

Fig. A1. Example beam map generated during the calibration of ADP M685 on 23 March 2011. The color scale depicts recorded acoustic backscatter in decibels. The number 80 refers to the maximum ABS recorded during the calibration from a point near the center of the beam.

is suspended by monofilament into the pool from the X–Y stepper motor stage so that the ball can be moved in a 1 m^2 grid perpendicular to the beam axis.

A Matlab script controls the position of the target sphere in the X–Y grid via serial commands to the motor controller. The Matlab script also controls when the ADP pings the target, and records the post-ping ABS from the target. The script systematically moves the target through a 5 cm grid spaced series of positions (i.e., 400 positions total), and records ABS from 3 pings at each of these positions. The script then determines the likely center of the acoustic beam and records pings from a finer resolution (2 cm grid spacing), additional 100 positions centered on this location. After finishing this second grid pattern, the script determines the maximum backscatter measured by the ADP at the center of the beam.

Beam pattern

Since the *Spray* ADP uses a simple circular monostatic transducer, the resulting beam pattern recorded during the calibration should be circular. The beam map also allows calculation of the half-power beamwidth, or two times the angle off-axis that the recorded beam strength drops by 3 dB. We found that the beam strength dropped by 3 dB approximately 9 cm off-axis. Given the 5 m distance to the target, the half-power beamwidth angle is equal to atan(0.18/5), or 2°.

Maximum ABS from a known target

In order to track instrument drift over time in any particular ADP, and to ensure comparability between different ADP instruments, we recorded the maximum return from the target for each beam for each ADP before and after deployment at sea.

References

Ainley, D.G., Dugger, K.D., Ford, R.G., Pierce, S.D., Reese, D.C., Brodeur, R.D., Tynan, C.T., Barth, J.A., 2009. Association of predators and prey at frontal features in the California Current: competition, facilitation, and co-occurrence. Marine Ecology Progress Series 389, 271–294.

Aksnes, D.L., Ohman, M.D., Riviere, P., 2007. Optical effect on the nitracline in a coastal upwelling area. Limnology and Oceanography 52, 1179–1187.

Andersen, V., Devey, C., Gubanova, A., Picheral, M., Melnikov, V., Tsarin, S., Prieur, L., 2004. Vertical distributions of zooplankton across the Almeria–Oran frontal zone (Mediterranean Sea). Journal of Plankton Research 26, 275–293.

Ashjian, C.J., Smith, S.L., Flagg, C.N., Idrisi, N., 2002. Distribution, annual cycle, and vertical migration of acoustically derived biomass in the Arabian Sea during 1994–1995. Deep Sea Research Part II 49, 2377–2402.

Bost, C.A., Cotte, C., Bailleul, F., Cherel, Y., Charrassin, J.B., Guinet, C., Ainley, D.G., Weimerskirch, H., 2009. The importance of oceanographic fronts to marine birds and mammals of the southern oceans. Journal of Marine Systems 78, 363–376.

Chelton, D.B., 1982. Large-scale response of the California Current to forcing by the wind stress curl. CalCOFI Reports 23, 130–148.

Chelton, D.B., Bernal, P.A., McGowan, J.A., 1982. Large-scale interannual physical and biological interaction in the California Current. Journal of Marine Research 40, 1095–1125.

Cullen, J.J., Eppley, R.W., 1981. Chlorophyll maximum layers of the Southern California Bight and possible mechanisms of their formation and maintenance. Oceanologica Acta 4, 23–32.

Cullen, J.J., Lewis, M.R., 1995. Biological processes and optical measurements near the sea surface: some issues relevant to remote sensing. Journal of Geophysical Research: Oceans 100, 13255–13266.

Davis, R.E., Ohman, M.D., Rudnick, D.L., Sherman, J.T., Hodges, B., 2008. Glider surveillance of physics and biology in the southern California Current System. Limnology and Oceanography 53, 2151–2168.

Davison, P., 2011. The specific gravity of mesopelagic fish from the northeastern Pacific Ocean and its implications for acoustic backscatter. ICES Journal of Marine Science 68, 2064–2074.

De Robertis, A., Jaffe, J.S., Ohman, M.D., 2000. Size-dependent visual predation risk and the timing of vertical migration in zooplankton. Limnology and Oceanography 45, 1838–1844.

Denman, K.L., Abbott, M.R., 1994. Time scales of pattern evolution from cross-spectrum analysis of advanced very high-resolution radiometer and coastal zone color scanner imagery. Journal of Geophysical Research: Oceans 99, 7433–7442.

D'Ovidio, F., De Monte, S., Alvain, S., Dandonneau, Y., Lévy, M., 2010. Fluid dynamical niches of phytoplankton types. Proceedings of the National Academy of Sciences, USA 107, 18366–18370.

Eggleston, D.B., Armstrong, D.A., Elis, W.E., Patton, W.S., 1998. Estuarine fronts as conduits for larval transport: hydrodynamics and spatial distribution of Dungeness crab postlarvae. Marine Ecology Progress Series 164, 73–82.

Flagg, C.N., Smith, S.L., 1989. On the use of the acoustic Doppler current profiler to measure zooplankton abundance. Deep-Sea Research 36, 455–474.

Franks, P.J.S., 1992. Sink or swim – accumulation of biomass at fronts. Marine Ecology Progress Series 82, 1–12.

Please cite this article in press as: Powell, J.R., Ohman, M.D. Changes in zooplankton habitat, behavior, and acoustic scattering characteristics across glider-resolved fronts in the Southern California Current System. Prog. Oceanogr. (2015), http://dx.doi.org/10.1016/j.pocean.2014.12.011

Gay, P.S., Chereskin, T.K., 2009. Mean structure and seasonal variability of the poleward undercurrent off southern California. Journal of Geophysical Research: Oceans 114.

Gorsky, G., Ohman, M.D., Picheral, M., Gasparini, S., Stemmann, L., Romagnan, J.B., Cawood, A., Pesant, S., Garcia-Comas, C., Prejger, F., 2010. Digital zooplankton image analysis using the ZooScan integrated system. Journal of Plankton Research 32, 285–303.

Haury, L.R., Venrick, E.L., Fey, C.L., McGowan, J.A., Niiler, P.P., 1993. The Ensenada Front: July 1995. CalCOFI Reports 34, 69–88.

Hayward, T.L., Venrick, E.L., 1998. Nearsurface pattern in the California Current: coupling between physical and biological structure. Deep-Sea Research Part II 45, 1617–1638.

Hickey, B.M., 1979. The California Current System—hypotheses and facts. Progress in Oceanography 8, 191–279.

Humston, R., Ault, J.S., Lutcavage, M., Olson, D.B., 2000. Schooling and migration of large pelagic fishes relative to environmental cues. Fisheries Oceanography 9, 136–146.

Johnston, T.M.S., Rudnick, D.L., 2014. Trapped diurnal internal tides, propagating semidiurnal internal tides, and mixing estimates in the California Current System from sustained glider observations, 2006–2012. Deep Sea Research Part II. http://dx.doi.org/10.1016/j.dsr2.2014.03.009.

Johnston, T.M.S., Rudnick, D.L., Pallas-Sanz, E., 2011. Elevated mixing at a front. Journal of Geophysical Research: Oceans 116. http://dx.doi.org/10.1029/2011jc007192.

Lampert, W., 1989. The adaptive significance of diel vertical migration of zooplankton. Functional Ecology 3, 21–27.

Lavaniegos, B.E., Ohman, M.D., 2007. Coherence of long-term variations of zooplankton in two sectors of the California Current System. Progress in Oceanography 75, 42–69.

Lefevre, J., 1986. Aspects of the biology of frontal systems. Advances in Marine Biology 23, 163–299.

Mackas, D.L., Washburn, L., Smith, S.L., 1991. Zooplankton community pattern associated with a California Current cold filament. Journal of Geophysical Research: Oceans 96, 14781–14797.

Marchesiello, P., McWilliams, J.C., Shchepetkin, A., 2003. Equilibrium structure and dynamics of the California Current System. Journal of Physical Oceanography 33, 753–783.

Martin, A.P., 2003. Phytoplankton patchiness: the role of lateral stirring and mixing. Progress in Oceanography 57, 125–174.

McClatchie, S., Cowen, R., Nieto, K., Greer, A., Luo, J.Y., Guigand, C., Demer, D., Griffith, D., Rudnick, D., 2012. Resolution of fine biological structure including small narcomedusae across a front in the Southern California Bight. Journal of Geophysical Research: Oceans 117, C04020. http://dx.doi.org/10.1029/2011JC007565.

Medwin, H., Clay, C.S., 1998. Fundamentals of Acoustical Oceanography. Academic Press, Boston.

Morel, A., 1988. Optical modeling of the upper ocean in relation to its biogenous matter content (case-I waters). Journal of Geophysical Research: Oceans 93, 10749–10768.

Mullin, M.M., 1998. Biomasses of large-celled phytoplankton and their relation to the nitricline and grazing in the California Current System off southern California, 1994–1996. CalCOFI Reports 39, 117–123.

Munger, L.M., Camacho, D., Havron, A., Campbell, G., Calambokidis, J., Douglas, A., Hildebrand, J., 2009. Baleen whale distribution relative to surface temperature and zooplankton abundance off Southern California, 2004–2008. CalCOFI Report 50, 155–168.

Munk, P., Hansen, B.W., Nielsen, T.G., Thomsen, H.A., 2003. Changes in plankton and fish larvae communities across hydrographic fronts off West Greenland. Journal of Plankton Research 25, 815–830.

Ohman, M.D., 1990. The demographic benefits of diel vertical migration by zooplankton. Ecological Monographs 60, 257–281.

Ohman, M.D., Wilkinson, J., 1989. Comparative standing stocks of mesozooplankton and macrozooplankton in the southern sector of the California Current System. Fishery Bulletin 87, 967–976.

Ohman, M.D., Drits, A.V., Clarke, M.E., Plourde, S., 1998. Differential dormancy of co-occurring copepods. Deep-Sea Research 45, 1709–1740.

Ohman, M.D., Powell, J.R., Picheral, M., Jensen, D.W., 2012. Mesozooplankton and particulate matter responses to a deep-water frontal system in the southern California Current System. Journal of Plankton Research 34, 815–827.

Ohman, M.D., Rudnick, D.L., Chekalyuk, A., Davis, R.E., Feely, R.A., Kahru, M., Kim, H.-J., Landry, M.R., Martz, T.R., Sabine, C., Send, U., 2013. Autonomous ocean measurements in the California Current Ecosystem. Oceanography 26, 18–25.

Pearcy, W.G., Krygier, E.E., Mesecar, R., Ramsey, F., 1977. Vertical distribution and migration of oceanic micronekton off Oregon. Deep-Sea Research 24, 223–245.

Pingree, R.D., Pugh, P.R., Holligan, P.M., Forster, G.R., 1975. Summer phytoplankton blooms and red tides along tidal fronts in the approaches to the English Channel. Nature 258, 672–677.

Polovina, J.J., Howell, E., Kobayashi, D.R., Seki, M.P., 2001. The transition zone chlorophyll front, a dynamic global feature defining migration and forage habitat for marine resources. Progress in Oceanography 49, 469–483.

Polovina, J.J., Balazs, G.H., Howell, E.A., Parker, D.M., Seki, M.P., Dutton, P.H., 2004. Forage and migration habitat of loggerhead (*Caretta caretta*) and olive ridley (*Lepidochelys olivacea*) sea turtles in the central North Pacific Ocean. Fisheries Oceanography 13, 36–51.

Postel, L., da Silva, A.J., Mohrholz, V., Lass, H.U., 2007. Zooplankton biomass variability off Angola and Namibia investigated by a lowered ADCP and net sampling. Journal of Marine Systems 68, 143–166.

Powell, J.R., 2013. Ocean fronts in the Southern California Current System and their role in structuring zooplankton distributions, diel vertical migration, and size composition. Ph.D. thesis. Univ. of Calif., San Diego.

Powell, J.R., Ohman, M.D., 2012. Use of glider-class acoustic Doppler profilers for estimating zooplankton biomass. Journal of Plankton Research 34, 563–568.

Powell, J.R., Ohman, M.D., 2015. Co-variability of zooplankton gradients with glider-detected density fronts in the Southern California Current System. Deep Sea Research Part II. http://dx.doi.org/10.1016/j.dsr2.2014.04.002.

Ries, L., Fletcher, R.J., Battin, J., Sisk, T.D., 2004. Ecological responses to habitat edges: mechanisms, models, and variability explained. Annual Review of Ecology, Evolution, and Systematics 35, 491–522.

Rykaczewski, R.R., Checkley, D.M., 2008. Influence of ocean winds on the pelagic ecosystem in upwelling regions. Proceedings of the National Academy of Sciences, USA 105, 1965–1970.

Sherman, J., Davis, R.E., Owens, W.B., Valdes, J., 2001. The autonomous underwater glider "Spray". IEEE Journal of Oceanic Engineering 26, 437–446.

Simpson, J.J., 1984. El Nino-induced onshore transport in the California Current during 1982–3. Geophysical Research Letters 11, 233–236236.

Smith, S.L., Lane, P.V.Z., 1991. The jet off Point Arena, California: its role in aspects of secondary production in the copepod *Eucalanus californicus* Johnson. Journal of Geophysical Research: Oceans 96, 14849–14858.

Smith, S.L., Jones, B.H., Atkinson, L.P., Brink, K.H., 1986. Zooplankton in the upwelling fronts off Pt. Conception, California, p. 195–213. In: Nihoul, J.D.J. (Ed.), Marine Interfaces Ecohydrodynamics: Proceedings of the 17th International Liège Colloquium on Ocean Hydrodynamics, Elsevier Oceanography Series, p. 42.

Sournia, A., 1994. Pelagic biogeography and fronts. Progress in Oceanography 34, 109–120.

Stanton, T.K., Chu, D.Z., Wiebe, P.H., 1998. Sound scattering by several zooplankton groups. II. Scattering models. Journal of the Acoustical Society of America 103, 236–253.

Todd, R.E., Rudnick, D.L., Mazloff, M.R., Davis, R.E., Cornuelle, B.D., 2011. Poleward flows in the southern California Current System: glider observations and numerical simulation. Journal of Geophysical Research: Oceans 116, C02026. http://dx.doi.org/10.1029/2010JC006536.

Venrick, E.L., 2002. Floral patterns in the California Current System off southern California: 1990–1996. Journal of Marine Research 60, 171–189.

Venrick, E.L., 2009. Floral patterns in the California Current: the coastal-offshore boundary zone. Journal of Marine Research 67, 89–111.

Wiebe, P.H., Morton, A.W., Bradley, A.M., Backus, R.H., Craddock, J.E., Barber, V., Cowles, T.J., Flierl, G.R., 1985. New developments in the Mocness, an apparatus for sampling zooplankton and micronekton. Marine Biology 87, 313–323.

Please cite this article in press as: Powell, J.R., Ohman, M.D. Changes in zooplankton habitat, behavior, and acoustic scattering characteristics across glider-resolved fronts in the Southern California Current System. Prog. Oceanogr. (2015), http://dx.doi.org/10.1016/j.pocean.2014.12.011